

AD A140004

XeF PUMPED Tm:YLF LASER SCALING

Final Report For:
1 April 1980 - 31 May 1981
CONTRACT N00014-80-C-0444

Prepared for:

OFFICE OF NAVAL RESEARCH
Department of the Navy
800 N. Quincy Street
Arlington, Virginia 22217

Prepared by:

Defense and Information
Systems Division
Federal Systems Group



SANDERS

30 CANAL STREET NASHUA, NEW HAMPSHIRE 03051

APR 12 1984

A

DTIC FILE COPY

20000802068

Reproduced From
Best Available Copy


XeF PUMPED Tm:YLF LASER SCALING

Final Report For:
1 April 1980 - 31 May 1981
CONTRACT N00014-80-C-0444

Prepared for:

OFFICE OF NAVAL RESEARCH
Department of the Navy
800 N. Quincy Street
Arlington, Virginia 22217

Prepared by:

Defense and Information
Systems Division
Federal Systems Group
 **SANDERS**
85 CANAL STREET - NASHUA, NEW HAMPSHIRE 03061



Accession For	
Form 6041	
1. TITLE	
2. AUTHOR	
3. SUBJECT	
4. ABSTRACT	
5. NOTES	
6. REFERENCES	
7. DISTRIBUTION	
8. SECURITY CLASS	
9. DATE OF	
10. CONTROL	
AI	

UNCLASSIFIED

SECURITY CLASSIFICATION OF THIS PAGE (When Data Entered)

REPORT DOCUMENTATION PAGE		READ INSTRUCTIONS BEFORE COMPLETING FORM
1. REPORT NUMBER	2. GOVT ACCESSION NO. ADP40006	3. REPORTING CATALOG NUMBER
4. TITLE (and Subtitle) XeF PUMPED Tm:YLF LASER SCALING		5. TYPE OF REPORT & PERIOD COVERED FINAL 1 April 1980-31 May 1981
7. AUTHOR(s) E.P. Chicklis, J. Baer, M. Knights, J. McCarthy		6. PERFORMING ORG. REPORT NUMBER
9. PERFORMING ORGANIZATION NAME AND ADDRESS SANDERS ASSOCIATES, INC. Defense and Information Systems Division 95 Canal St., Nashua, New Hampshire 03061		8. CONTRACT OR GRANT NUMBER(s) N00014-80-C-0444
11. CONTROLLING OFFICE NAME AND ADDRESS Office of Naval Research, Dept. of the Navy 800 N. Quincy St., Arlington, VA 22217		12. REPORT DATE February 1984
14. MONITORING AGENCY NAME & ADDRESS (if different from Controlling Office)		13. NUMBER OF PAGES 84
		15. SECURITY CLASS. (of this report) UNCLASSIFIED
		16. DECLASSIFICATION/DOWNGRADING SCHEDULE
16. DISTRIBUTION STATEMENT (of this Report) <div style="border: 1px solid black; padding: 5px; margin: 10px auto; width: fit-content;"> This report is the property of the Department of the Navy and is loaned to you. It and its contents are not to be distributed outside your agency. </div>		
17. DISTRIBUTION STATEMENT (of the abstract entered in Block 20, if different from Report)		
18. SUPPLEMENTARY NOTES		
19. KEY WORDS (Continue on reverse side if necessary and identify by block number) Tm:YLF Laser Resonant Pumped Laser Blue Laser Solid State Laser		
20. ABSTRACT (Continue on reverse side if necessary and identify by block number) <p>Laser operation in the $^1D_2 - ^3F_4$ transition at $\lambda = 450\text{nm}$ pumped by XeF is described. The experiments were carried out using a 1 meter e-beam pumped XeF laser. Oscillator and amplifier experiments were carried out, the measured Tm³⁺:YLF amplifier gain is in good agreement with that predicted by a "pump-while extract" model of a loss-less Tm:YLF amplifier.</p> <p style="text-align: right;">-Over-</p>		

DD FORM 1 JAN 73 1473 EDITION OF 1 NOV 65 IS OBSOLETE

UNCLASSIFIED

SECURITY CLASSIFICATION OF THIS PAGE (When Data Entered)

UNCLASSIFIED

SECURITY CLASSIFICATION OF THIS PAGE(When Data Entered)

The maximum Tm:YLF laser output observed on this program was ~100mJ; attainment of higher output levels was limited by experimental difficulties.

UNCLASSIFIED

SECURITY CLASSIFICATION OF THIS PAGE(When Data Entered)

FOREWARD

This report describes work on the Tm^{3+} :YLF laser carried out by Sanders Associates between 1 April 1980 and 31 May 1981. Tm :YLF is a resonantly pumped, crystalline solid state laser which emits nominally at 450nm when pumped by the XeF rare gas halide laser. This system was first demonstrated by Sanders Associates in 1978 under DoE support. Prior to the start of this program approximately 1mJ had been extracted from a Tm :YLF laser.

TABLE OF CONTENTS

	<u>Page</u>
1.0 INTRODUCTION	1
1.1 Background	1
1.2 Program Objectives and Goals	1
1.3 Results	3
2.0 RESONANT PUMPED LASER MODEL, Tm:YLF SPECTROSCOPY AND CONVERSION EFFICIENCY CODE	4
2.1 Introduction	4
2.2 Resonant Pumping	4
2.3 Spectroscopy	8
2.3.1 Emission Cross Section	8
2.3.2 Level Diagram	8
2.3.3 Upper Level Lifetime	8
2.3.4 Absorption Coefficients	8
2.3.5 Intermediate State Lifetimes	8
2.4 Tm:YLF Laser Code	14
3.0 EXPERIMENTAL RESULTS	20
3.1 Introduction	20
3.2 Design Requirements	20
3.2.1 Longitudinal Pumping	21
3.2.2 Transverse Pumping	22
3.3 Initial Experiments	34
3.3.1 Beam Profiling	34
3.3.2 Damage Testing	38
3.3.3 Oscillator Experiments	38
3.4 Design Improvement	41
3.4.1 Optical Integrators	41
3.4.2 Transverse	42

TABLE OF CONTENTS (Cont'd.)

	<u>Page</u>
3.5 October Experiments	44
3.5.1 Experiment Objectives	44
3.5.2 Oscillator Experiments - Diagnostics	50
3.5.3 Integrator Test	53
3.6 Amplifier Measurements	56
3.7 February Experiments	57
3.7.1 Set-Up	57
3.7.2 First Session with the XeF Laser	58
3.7.3 Modified Set-Up	62
3.7.4 Fail-Back Experiment	64
Discussion	64
Model	66
4.0 SUMMARY AND CONCLUSIONS	74
REFERENCES	75
APPENDIX A - Laser Amplifier Model	A-1

TABLE OF FIGURES

<u>Figure</u>	<u>Page</u>
2-1 Longitudinal Pumped Geometry Linear Downconversion	5
2-2 Tm:YLF 1D_2 Cross Section	9
2-3 Tm:YLF Energy Levels	10
2-4 1D_2 Initial Lifetime Versus Concentration	11
2-5 Wavelength Dependent Absorption of XeF Radiation	12
2-6 Levels involved in Tm $^{+3}$:YLF Laser	16
3-1 Primary Focusing Lens	23
3-2 Simple Transverse Pumping	25
3-3 Pentagonal Crystals	28
3-4A Irregular Pentagons	29
3-4B Irregular Pentagons	30
3-5 Prime Focus Profiling	35
3-6 Pump Beam Profiling	36
3-7 Lydex Exposures	37
3-8 Measured Damage Fluence	39
3-9 Integrator Experimental Layout	43
3-10 Equal Area Pentagons	45
3-11 New Transverse Crystal Design	46
3-12 A 0.45 cm 2 Transverse Pumping Crystal	47
3-13 Transverse Pumping Assembly with External Reflectors	48
3-14 Transverse Relay Optics	49
3-15 Oscillator Experiment, with Diagnostics	51
3-16 Input/Output Laser Pulses	52
3-17 Integrator Experiments	54
3-18 Beam Cross-Section Comparison	55

TABLE OF FIGURES (Cont'd.)

<u>Figure</u>	<u>Page</u>
3-19 Integrator Experiments	59
3-20 Amplifier Experiment - AERL Floor Plan Jun - Apr 1981	60
3-21 Amplifier Experiment	63
3-22 Levels Involved in Tm^{+3} :YLF Laser	67
3-23 Amplifier Models	69
3-24 Computer Amplifier Model	70
3-25 Tm :YLF 1D_2 Cross-Section	73

TABLE OF TABLES

<u>Table</u>	<u>Page</u>
2-1 Tm:YLF Parameters	7
2-2 Tm:YLF Lifetimes	13
2-3 Tm:YLF Laser Kinetics Equation	17
3-1 Transverse Pumped Design Parameters	26
3-2 Fraction of Input Energy Deposited in Irregular Pentagons	31
3-3 Stored Energy	33
3-4 Dye Laser Seeded - Tm:YLF Amplifier Data	65
3-5 Results - π Line 452.7 nm, $\Delta\lambda = 1.2$ nm FWHM	71
3-6 Results - σ Line 452.6 nm, $\Delta\lambda = 0.8$ nm FWHM π Line 448.5 nm, $\Delta\lambda = 0.5$ nm FWHM	72
A-1 Pump-While-Extract Program Listing	A-3

1.0 INTRODUCTION

1.1 BACKGROUND

(SLC)
→ The laser requirements (energy per pulse, average power, beam quality) for the ground based Strategic Laser Communications mission represent a significant advance over currently available technology. The combination of very high average power and near diffraction limited beam quality in a spectral region where comparatively few devices have been developed poses a severe challenge to the technology.

This report describes work on the Tm^{3+} :YLF laser carried out by Sanders Associates between 1 April 1980 and 31 May 1981. A Tm :YLF laser is a resonantly pumped, crystalline solid state laser, which emits nominally at 450nm when pumped by the XeF rare gas halide laser. This system was first demonstrated by Sanders Associates in 1978 under DoE support. Prior to the start of this program approximately 1mJ had been extracted from a Tm :YLF laser.

1.2 PROGRAM OBJECTIVES AND GOALS

The performance goals of this program were as follows:

Energy per pulse: 1J

Conversion Efficiency: 30%

→ The technical objective of this program was the determination of the feasibility of XeF pumped Tm :YLF as a source for the SLC ground based mission. At the start of the program three crucial issues remained to be resolved:

a. Internal Losses

Based on the spectroscopic and material properties of Tm :YLF the efficiency and pulse energy required for the SLC mission appear feasible. However in previous work validation of the theoretical relationship between gain and pump fluence was not obtained, that is, the possibility of loss mechanisms in Tm :YLF had not been resolved.

Fortunately, in a resonant pumped laser the relationship between gain and pump fluence is a simple one and can be measured in a conceptually straightforward way.

b. Optical Coupling

Although the internal conversion efficiency of Tm:YLF (based on the spectroscopic parameters) is high, the overall system efficiency requirements demand high coupling efficiency and high extraction efficiency. A key issue to be resolved is whether a practical high power system can be built using a single aperture XeF laser pumping a solid state laser while maintaining sufficiently high pump fluence for adequate gain with the additional constraint of high pump absorption.

c. High Average Power Operation with Near Diffraction Limited Beam Quality

High average power solid state lasers are subject to thermal induced optical distortion which can limit the power extracted with good beam quality. Feasibility assessment of a high average power, high efficiency Tm:YLF laser with near diffraction limited beam quality was a key technical issue of this program.

In order to satisfy this technical objective the following technical goals were adopted:

(a) Experimental determination of the system gain as function of pumping fluence to determine whether or not the Tm³⁺:YLF exhibited unanticipated loss mechanisms,

(b) Experimental demonstration of a Tm:YLF oscillator or amplifier for which efficient absorption of the pump radiation is obtained under conditions for which the system gain coefficient is suitable for efficient extraction,

(c) Conceptual design of a high power, high efficiency Tm:YLF laser operating with near diffraction limited beam quality.

1.3 RESULTS

The key results of this program were:

a. The measured gain at $\lambda = 2.7\text{nm}$ is in good agreement with the gain calculated from a "pump-while-extract" model using the measured pump fluence, absorption coefficient, pulsewidth, T_m decay rate, and T_m emission cross-section. The laser properties for $Tm:YLF$ are adequately described with an emission cross-section of $\beta\sigma = 2.5 \times 10^{-20}\text{cm}^2$.

b. Efficient optical coupling of XeF lasers to $Tm:YLF$ was achieved at pumping levels for which a gain coefficient, $g_0 \sim 0.1\text{cm}^{-1}$, was measured. This corresponds to a stored energy density of $1.7\text{J}/\text{cm}^3$; these values of gain coefficient and stored energy density are ideally suited for a high power system.

c. Nearly lossless concentration of the highly multimode XeF pump laser was demonstrated using a modified commercially available "beam integrator". Fluence concentrations of $\sim 100:1$ was demonstrated with a very high degree of beam uniformity.

d. Efficient extraction of the stored energy was not, however, obtained. This was due to experimental difficulties, particularly the lack of reliability of the XeF pump laser. Approximately 100mJ was extracted from a $Tm^{3+}:YLF$ amplifier with an extracting fluence well below E_{sat} .

2.0 RESONANT PUMPED LASER MODEL, Tm:YLF SPECTROSCOPY and CONVERSION EFFICIENCY CODE

2.1 INTRODUCTION

This section describes the static model of a linear downconverter (resonant pumped laser), the spectroscopy of Tm:YLF, and the calculated conversion efficiency of Tm:YLF using the static model and the full rate equation analysis of a Tm:YLF oscillator.

2.2 RESONANT PUMPING

The term resonantly pumped laser is used to describe the general phenomenon of narrow band pumping of a laser by another laser. In such systems, quantum efficiencies to the upper laser level approaching unity, are achieved with little energy waste or buildup time. This is contrasted with conventional flashlamp (i.e., broadband) pumped systems where the lasing level is populated by heat producing, time consuming, non-radiative decays from many higher lying levels. Such resonantly pumped systems have been demonstrated in several crystalline materials, whose outputs range from the UV as in KrF pumped Ce:YLF, to the IR, as in doubled Nd pumped Er:YLF.

Consider a simple system consisting of three states: ground state, lower laser level and upper laser level. We assume:

- a. The upper state lifetime is longer than the pump pulse (true for Tm:YLF with active ion concentrations <10%)
- b. The converter is pumped longitudinally with a plane wave and
- c. Most of the pump light is absorbed in a single pass through the crystal ($\alpha l > 2$).

All these assumptions reasonably describe the Tm:YLF system which is described previously.⁽¹⁾ The geometry is shown in Figure 2.1.

LONGITUDINAL PUMPED GEOMETRY LINEAR DOWNCONVERSION

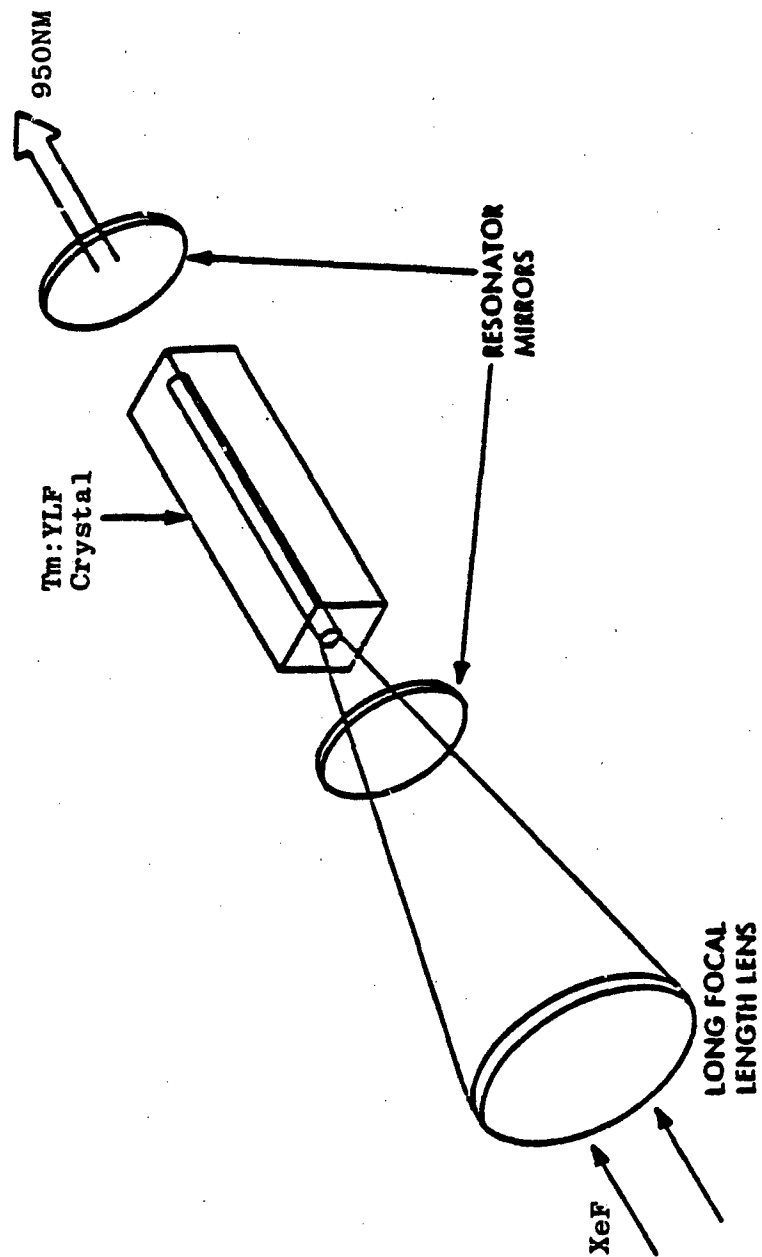


FIGURE 2-1

The inversion, $N^*(\text{cm}^{-3})$ at any point in the crystal is given by:

$$N^* = \frac{\alpha E_p}{h\nu}$$

where α is the absorption coefficient (cm^{-1}), E_p is the pump fluence (J/cm^2) and $h\nu$ the photon energy (joules). The gain at any point is given by:

$$g_o = N^* \beta \sigma$$

where σ is the stimulated emission cross section, and β is the occupation factor of the upper laser level.

Since the fluence is attenuated exponentially along the axis, the gain seen in a single pass along the axis is given by

$$\bar{g}_o l = \int_0^l g_o(x) dx = \frac{\alpha \beta \sigma}{h\nu} \int_0^l E_p(x) dx$$

and since $E_p(x) = E_f e^{-\alpha x}$

where E_f is the fluence at the face, we have

$$\bar{g}_o = \frac{\beta \sigma E_f}{h\nu l} [1 - e^{-\alpha l}] = \frac{\beta \sigma E_f}{h\nu l}$$

for $\alpha l \gg 1$.

Table 2-1 lists the pertinent parameters for Tm:YLF as well as some calculated values of the gain. Note that for 5% Tm:YLF $\alpha = 0.30 \text{cm}^{-1}$ and for a 6.0cm crystal (85% absorption)

$$\bar{g}_o = 0.12 \text{cm}^{-1}$$

with a face fluence of $15 \text{J}/\text{cm}^2$.

TABLE 2-1

Tm:YLF PARAMETERS

	3% Tm:YLF	5% Tm:YLF
$\alpha(\text{cm}^{-1})$.18	.30
$\beta\sigma(\text{cm}^2)$	3.2×10^{-20}	3.2×10^{-20}
$\frac{*}{g_0}$ at $E_f = 15\text{J}/\text{cm}^2$ with $l = 6\text{cm}$	0.09 cm^{-1}	0.12 cm^{-1}

$$\frac{*}{g_0} = \frac{\beta\sigma E_f}{h\nu l} \left\{ 1 - e^{-\alpha l} \right\}$$

$$h\nu(353) = 5.6 \times 10^{-19} \text{ J/photon}$$

2.3 SPECTROSCOPY

This section summarizes the spectroscopic parameters of Tm:YLF measured in this and previous programs.⁽¹⁾

2.3.1 EMISSION CROSS SECTION

The emission cross section for the π and σ components are shown in Figure 2-2.

2.3.2 LEVEL DIAGRAM

The energy levels of the upper and lower laser levels are shown in Figure 2-3.

2.3.3 UPPER LEVEL LIFETIME

1D_2 lifetime at 300K vs Tm concentration is shown in Figure 2-4.

2.3.4 ABSORPTION COEFFICIENTS

The absorption coefficient of Tm:YLF vs wavelength in the region of XeF emission is shown in Figure 2-5.

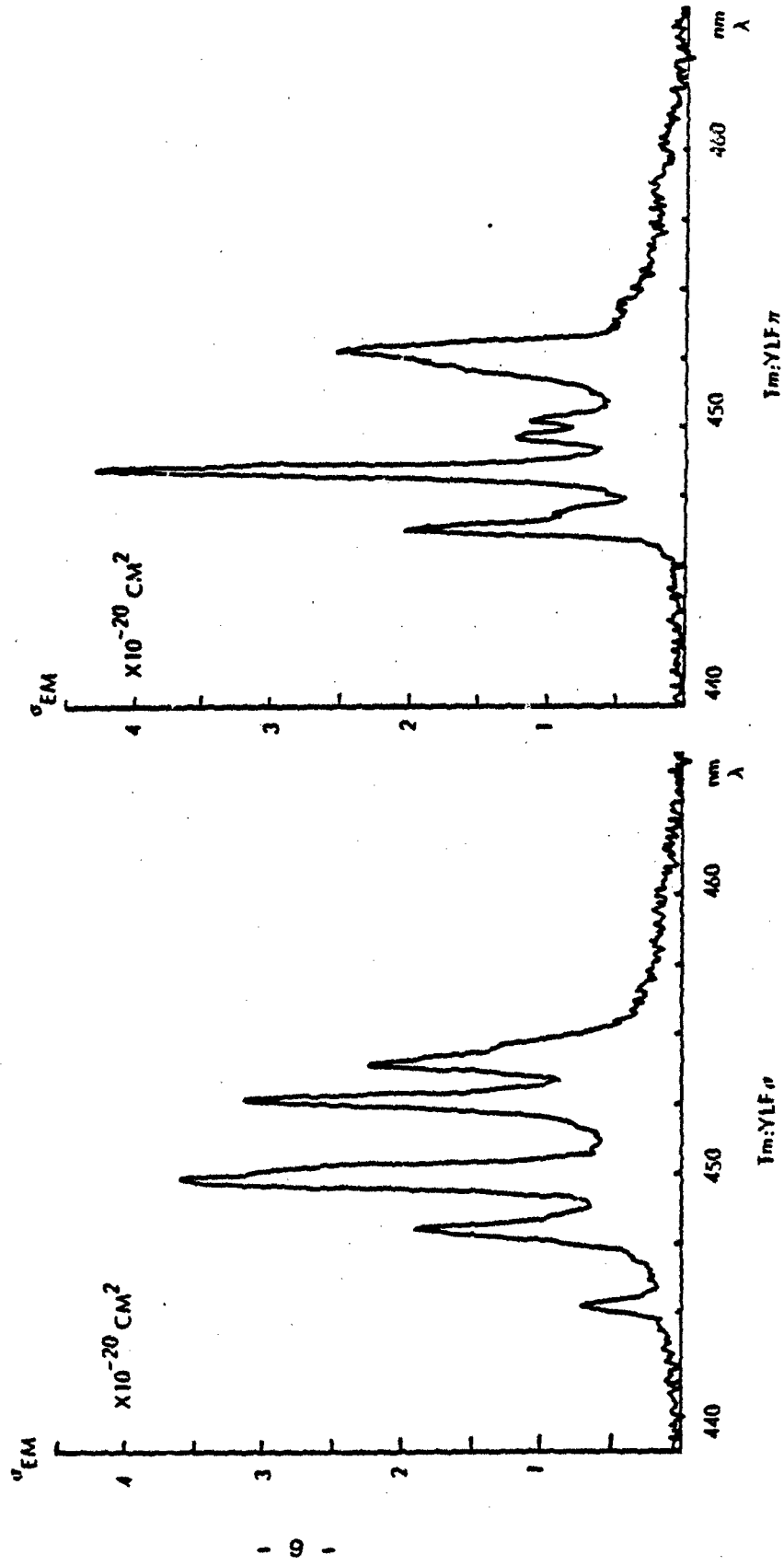
2.3.5 INTERMEDIATE STATE LIFETIMES

Fluorescence lifetimes of all the states up to 1D_2 were measured and are reported in Table 2-2. These data were used as input to a rate equation model of a Tm:YLF laser which includes possible interaction between all the excited states of Tm:YLF described in Table 2-2.

010 555 010 000 100 100 200 300 400 500 600 700 800 900 1000 1100 1200 1300 1400 1500 1600 1700 1800 1900 2000 2100 2200 2300 2400 2500 2600 2700 2800 2900 3000 3100 3200 3300 3400 3500 3600 3700 3800 3900 4000 4100 4200 4300 4400 4500 4600 4700 4800 4900 5000 5100 5200 5300 5400 5500 5600 5700 5800 5900 6000 6100 6200 6300 6400 6500 6600 6700 6800 6900 7000 7100 7200 7300 7400 7500 7600 7700 7800 7900 8000 8100 8200 8300 8400 8500 8600 8700 8800 8900 9000 9100 9200 9300 9400 9500 9600 9700 9800 9900 10000



1 Tm:YLF D CROSS SECTION 2



07199-15
 07199-16

FIGURE 2-2



Defensive
Systems
Division

Tm:YLF ENERGY LEVELS

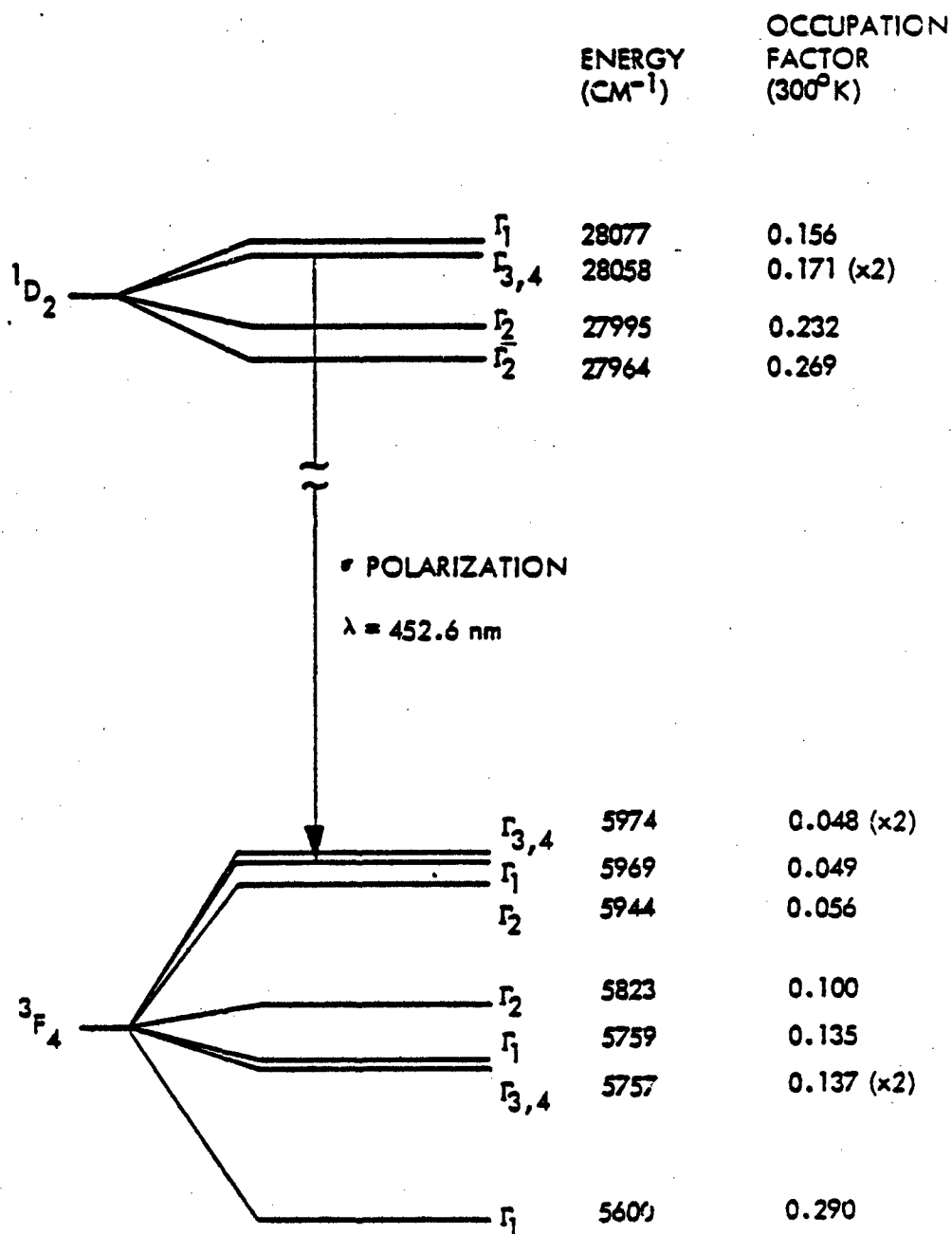
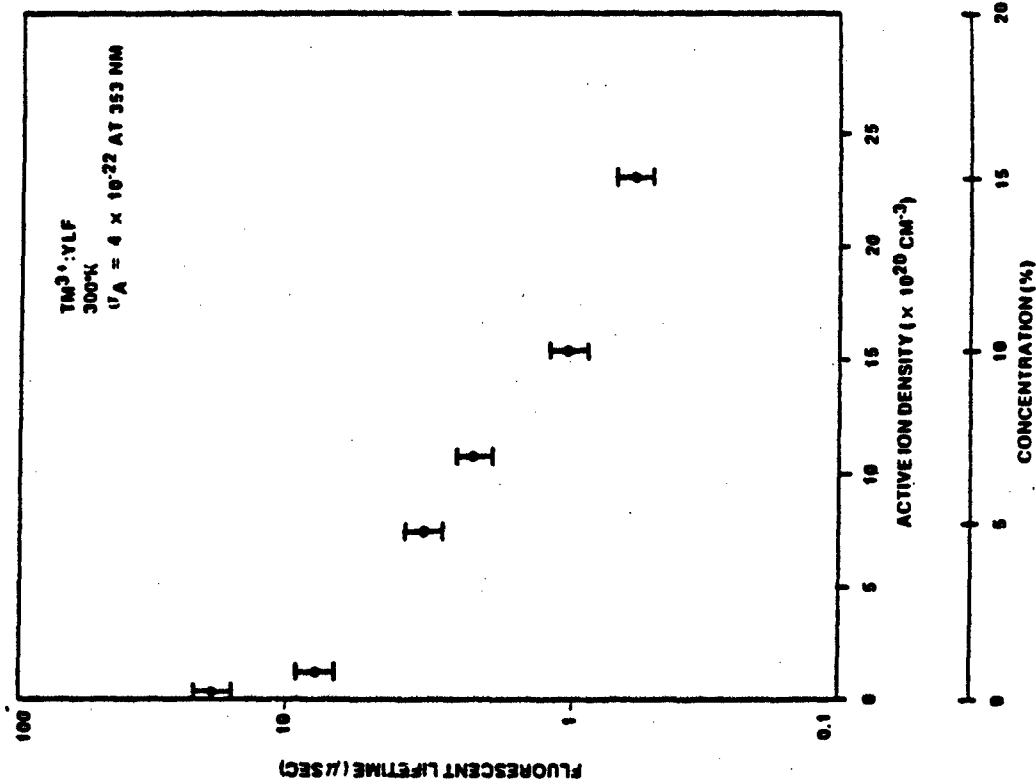


FIGURE 2-3

Defensive Systems Division
Federal Systems Group



ID₂ INITIAL LIFETIME VERSUS CONCENTRATION



07151-10

FIGURE 2-4

Defensive Systems Division
Federal Systems Group



SANDERS

WAVELENGTH DEPENDENT ABSORPTION OF XeF RADIATION

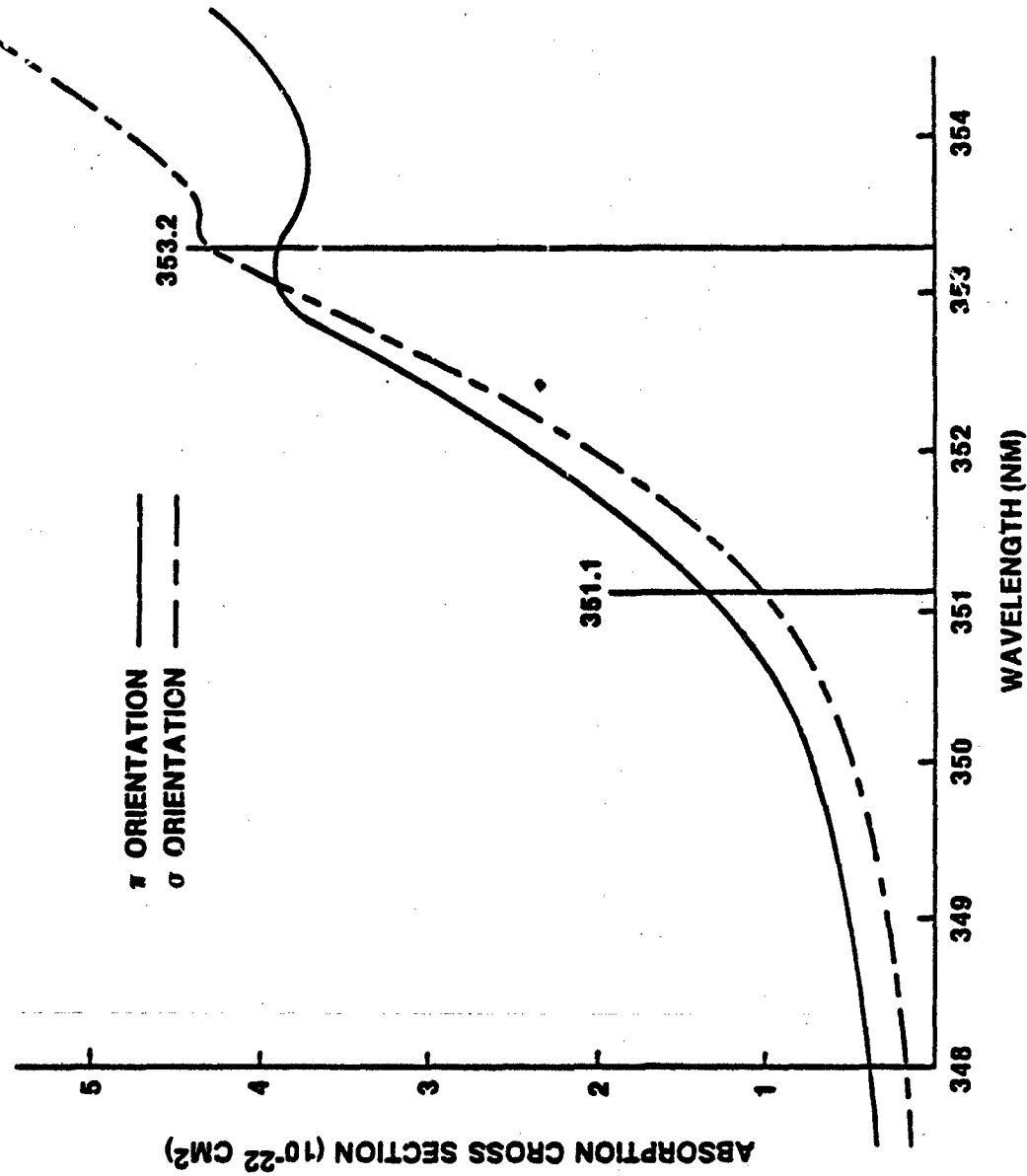


FIGURE 2-5

06011-10

TABLE 2-2

Tm:YLF LIFETIMES

MANIFOLD	THEORY	DOPANT						
		1/2%	1%	5%	7%	10%	15%	
1D_2		18.8	7.82	3.16	2.15	0.96	0.56	μsec
1G_4	10^3	806	280	12.2		4.13	2.13	μsec
3F_2	.18							μsec
3F_3	16	.5						μsec
3H_4		1800	1230	77	28.5	8.2	3.3	μsec
* 3F_4		15	14	7.5		6.0		msec

* The lifetime of this state is dominated by impurities and the measured variation shown is probably not related to Tm^{3+} concentration.

2.4 Tm:YLF LASER CODE

To establish design parameters for the conversion efficiency experiments, a computer model of the Tm:YLF system was developed. The purpose of this simulation is to obtain a first order approximation of laser performance based on known parameters. From this information major problems or difficulties can be predicted prior to the initiation of the experiments at AVCO.

The computer simulation uses a model of the Tm^{+3} ion in YLF that accounts for all the pertinent interactions, either known or conjectured, between the populations of the nine manifolds and the laser photon flux. These interactions are of four types:

- Transitions between two manifolds, induced by absorption of a photon, either pump or laser.
- Transitions between two manifolds induced by spontaneous fluorescence or spontaneous non-radiative decay.
- Multiple ion effects wherein two ions in appropriate manifolds transition to the other two manifolds.
- Transition between two manifolds as a result of stimulated emission of a laser photon.

The behavior of each of the ten populations of interest is modelled by using a representative differential equation to describe the rate of change of the instantaneous populations involved. There are forty possible elements to each equation. Most of the elements, however, such as stimulated emission from low lying manifolds are either zero or negligibly small, and therefore can be eliminated. As a result, all equations display as a maximum eight elements.

Further simplification in the rate equations can be made based on the following assumptions. (See Figure 2-6.)

- No pertinent interaction occurs within the 3H_5 manifold
- The pump laser can be treated by a source term in 1D_2 , designated as n_7 .
- The low percent of inverted ions will allow the assumption of the ground manifold population 3H_6 to be held constant.
- "Concentration Quenching" occurs at a rate r whenever there exists a resonance or near resonance between a populated excited state to a lower lying transition in one ion and a ground state to excited state transition in another ion.

The resulting equations are shown in Table 2-3. \dot{n} indicates a time derivative of ion concentration of each energy level. Due to conservation of mass, at any time $\sum_{n=8} \dot{n} = 0$. In addition to describing the rate of change in each level horizontally, the actual mechanism of concern is pointed out in vertical rows. The description of these mechanisms is as follows:

- Columns 1 and 3 describe the initial transition from ground state to the upper level, n_7 , upon absorption of the pump energy. The rate of transfer is proportional to number of pump photons absorbed per unit area, and inversely proportional to the length of crystal.

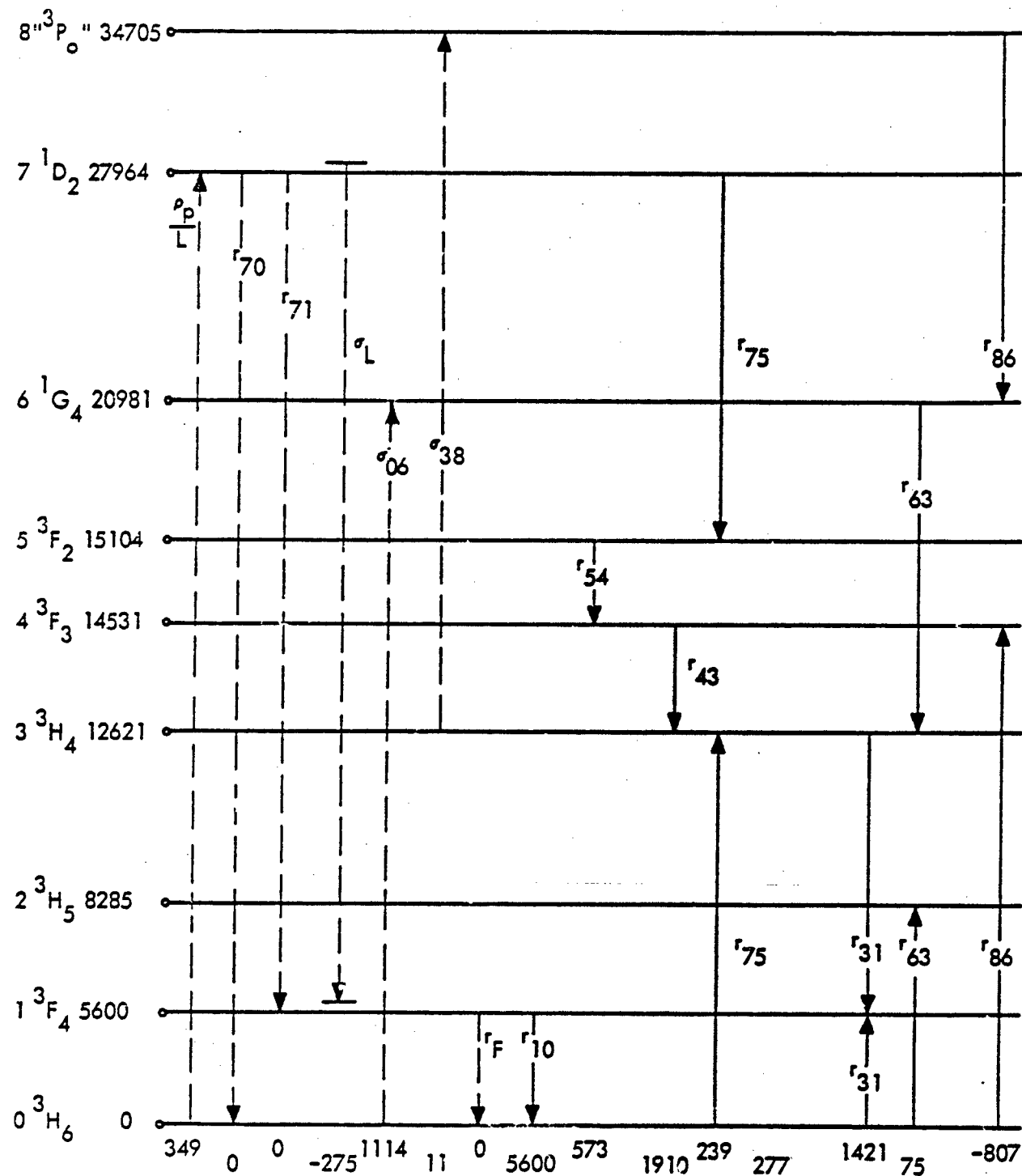
The third column indicates immediate decay processes after initial absorption.

- The second column represents the two competing processes in stimulated emission which involves the upper and lower



Defensive
Systems
Division

LEVELS INVOLVED IN Tm + ³YLF LASER



08110-2

FIGURE 2-6

TM:YLF LASER KINETICS EQUATION

TABLE 2-3

PUMP	LASER EMISSION	LASER ABSORPTION	FLUORESCENCE	CONCENTRATION QUENCHING
$\dot{n}_8 =$		$\rho_L \sigma_{38} n_3$		$- n_8 r_{86}$
$\dot{n}_7 = \rho_p \frac{1}{L_{XTAL}}$	$- \rho_L \sigma_L n_7 \beta_u + \rho_L \sigma_L n_1 \beta_L - n_7 r_{70} - n_7 r_{71}$			$- n_7 r_{75}$
$\dot{n}_6 =$		$\rho_L \sigma_{06} n_0$		$+ n_8 r_{86} - n_6 r_{63}$
$\dot{n}_5 =$			$- n_5 r_{59}$	$+ n_7 r_{75}$
$\dot{n}_4 =$			$+ n_5 r_{59} - n_4 r_{43} + n_8 r_{86}$	
$\dot{n}_3 =$		$- \rho_L \sigma_{38} n_3$	$+ n_4 r_{43}$	$+ n_7 r_{75} + n_6 r_{63} - n_3 r_{31}$
$\dot{n}_2 = 0$				
$\dot{n}_1 =$	$+ \rho_L \sigma_L n_7 \beta_u - \rho_L \sigma_L n_1 \beta_L$		$- n_1 r_{10}$	$+ n_6 r_{63} + 2n_3 r_{31}$
$\dot{n}_0 = -\rho_p \frac{1}{L_{XTAL}}$	$- \rho_L \sigma_{06} n_0 + n_7 r_{70}$		$+ n_1 r_{10} - n_8 r_{86} - n_7 r_{75} - n_6 r_{63} - n_3 r_{31}$	
$\dot{n}_L = c \rho_L \left\{ \sigma_L n_7 \beta_u - \sigma_L n_1 \beta_L - \sigma_{06} n_0 - \sigma_{38} n_3 - \left[L_n (R_1 R_2) \right] (2L_{XTAL})^{-1} - \delta \right\} + n_7 r_{71} A$				

laser levels occupation factors, along with the two laser photon absorption mechanisms.

- The fourth column delineates all spontaneous interreaction such as fluorescent, i.e. radiative; or thermal, i.e. non-radiative.
- The fifth column illustrates the four known or conjectured (r_{63}) two ion interactions under Concentration Quenching, in a separate column each.

The composite equation, for the laser photon flux, contains three other terms unrelated to the above processes. There are distributed losses, both for the scattering in the crystal and the round trip loss induced by such things as mirror absorption and transmission. The last term deals with the contribution from fluorescence into the beam volume of the appropriate wavelength.

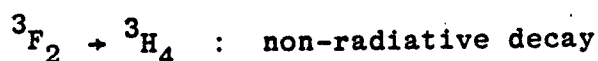
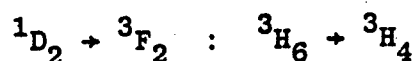
The predicted operation of the Tm:YLF laser has been determined with the above model. Conversion efficiency of the XeF laser energy was calculated to be about 40% with a pump energy flux of 15 to 20 J/cm² with the assumption that the loss term σ_{38} , is non-existent. σ_{38} is the absorption cross-section between the 3H_4 and 3P_0 multiplets. These multiplet widths are such that overlap between 3H_4 - 3P_0 absorption transition may be resonant with $^1D_2 \rightarrow ^3F_4$ emission transitions. This would represent a loss mechanism at the laser line of magnitude

$$N(^3H_4) \cdot \beta_1 \sigma_{38}^{ij}$$

where $N(^3H_4)$ is the instantaneous population of the 3H_4 multiplet, β_1 is the occupation factor of the i^{th} state in 3H_4 and σ_{38}^{ij} is the absorption cross-section between the i^{th} state of 3H_4 and the j^{th} of 3P_0 which coincides with any one of the $^1D_2 - ^3F_4$ transitions.

In the resonant pumped Tm:YLF laser the initial XeF excitation is absorbed by and stored in 1D_2 . In very dilute Tm concentration (<1%), 1D_2 decays primarily radiatively and predominantly to 3H_0 , 3F_4 , and 3H_5 , the 3H_4 population in this case is negligible and there is no loss to the $^1D_2 - ^3F_4$ lasing transitions.

At high Tm^{3+} concentration 1D_2 decays non-radiatively by "concentration quenching" via the ion-ion interactions:



A Tm ion initially excited to 1D_2 decays in this mode in a manner that results in two Tm ions excited to 3H_4 . Note that r_{54} and r_{43} are fast.

An estimate of the rate of this process (assuming it is the dominant 1D_2 decay mode) can be inferred from Figure 2-4 which shows the 1D_2 lifetime vs. concentration. 1D_2 decays non-exponentially and the cited values of lifetime refer to the initial \exp^{-1} decay of the population. The loss at any instant is:

$$\alpha_{38} = N(^3H_4)\sigma_{38}$$

On time scales short compared to the 1D_2 decay α_{38} will be negligible irrespective of the value of σ_{38} . Since the value of σ_{38} is not known (it could be zero) calculation of the 3H_4 population as a function of time were not carried out.

3.0 EXPERIMENTAL RESULTS

3.1 INTRODUCTION

The experimental program for Tm:YLF laser evaluation was carried out by Sanders at the Avco Everett Research Laboratories (AERL) using a 1 meter XeF laser as the pump. Design and fabrication of all the Tm:YLF experimental hardware was carried out at Sanders.

3.2 DESIGN REQUIREMENTS

Several oscillator designs ranging from simple single pass transverse pumped geometries to complex multipass geometries were carried out to optimize the pump absorption and maximize the conversion efficiency. In the design of resonant pumped lasers a few basic conditions must be met:

- (a) fluences must be maintained well below the damage limits of components, particularly coatings;
- (b) sufficient energy must be deposited in the crystal to assure sufficiently high gain for efficient extraction;
- (c) crystal length and concentration must be such that $\alpha l > 1$ (longitudinal pumping) with the constraints on α (active ion density) that the lifetime be longer than the pump pulse and in l that it be less than on the order of the depth of field of the image to eliminate vignetting of the pump beam.

To determine the fluence requirements we recall from Section 2.0 that the relationship between gain and pump fluence for a longitudinally pumped crystal was shown to be

$$\bar{g}_0 = \frac{\beta \sigma E_f}{h\nu l} \left(1 - e^{-\alpha l} \right);$$

and for typical experimental parameters (5%Tm:YLF, $l = 6$ cm)

$\bar{g}_0 = 0.08 \text{ cm}^{-1}$ at $E_f = 10 \text{ J/cm}^2$, where E_f is the fluence at the front face.

For oscillator experiments the optimal gain coefficient for efficient extraction depends on the ratio of internal losses to the coupling mirror "loss". In flashlamp pumped and resonant pumped laser oscillators typical values of the small signal gain coefficient for efficient extraction are $\sim 0.2 - 0.4 \text{ cm}^{-1(3)}$. This means that experiments must be designed to generate face fluences of $\sim 30 - 60 \text{ J/cm}^2$.

Discussions with AERL personnel indicated that little was known about the beam quality of the 1m XeF laser. The estimated divergence of the device was a few milliradians when operated at an output of 10J in an aperture of 85 x 85 mm.

Based on this initial information several design approaches were generated. In very simple terms there are two basic coupling approaches - transverse and longitudinal. In the former, a high pump absorption coefficient or multi pass pumping geometry is required to generate sufficient gain; in the latter the pump must be coupled through the rear resonator mirror. In both cases precise alignment must be maintained between the pumped volume and the resonator axis. We consider details of each approach below.

3.2.1 LONGITUDINAL PUMPING

In longitudinal pumping the pump laser is coupled to the crystal through the rear mirror of the Tm:YLF resonator and the pump beam is co-linear with the resonator axis. This approach has several advantages:

(a) Fabrication

Samples are simple to fabricate, sample shape is of no concern, and only two laser polished faces are required.

(b) Absorption

A 5% Tm:YLF sample exhibits an absorption coefficient of 0.31 cm^{-1} at 353 nm. The maximum practical Tm concentration is about 10% ($\alpha = 0.6 \text{ cm}^{-1}$) above which the $^1\text{D}_2$ lifetime is shorter than the pump pulse increasing the losses to non-

radiative decay. Thus path lengths of $\sim 6 - 10$ cm are required for efficient absorption in a single pass. This is readily obtained in longitudinal pumping geometry.

In addition, a longitudinally pumped oscillator is simple to model - gain is calculated from the face fluence and emission cross-section. The difficulties of longitudinal pumping are that the pump beam must pass through the rear reflector of the resonator and some care must be taken to prevent coating damage. Figure 3-1 shows the coupling lens purchased for longitudinal pumping experiments. The 550 mm focal length lens images a plane wave of divergence 10 mrad to a 5.5×5.5 mm diameter spot in the image plane. With a 10J input the fluence in the image plane is $>30\text{J}/\text{cm}^2$.

3.2.2 TRANSVERSE PUMPING

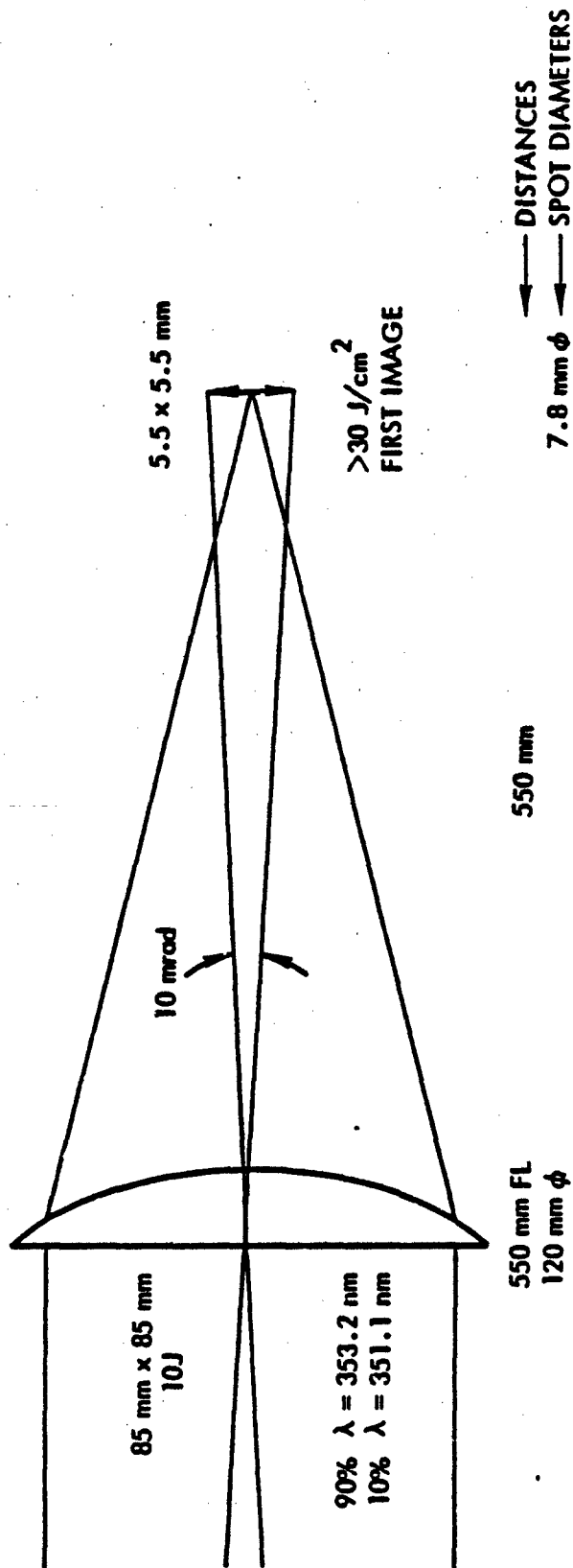
Because the $\text{Tm}:\text{YLF}$ laser will operate more efficiently the higher the gain, effort must be made to maximize the energy absorbed along the crystal axis. In longitudinal pumping, where the pump energy enters the crystal along the oscillator axis, this maximum is the point where the surface damage threshold of the crystal is reached. With slow focusing; i.e., $f/\#$ greater than three, the surface fluence and adsorbed energy are approximately equal so the limit on fluence is the limit on absorbed energy.

To avoid this limit one must break the relationship between surface fluence and energy on axis. Generally, such schemes involve transverse pumping. Unlike longitudinal pumping, the pump light now enters from the side, and floods the crystal, as it is no longer confined to the axis.

The first cut design would have a beam, below the surface damage threshold illuminating the side of a slab. For Tm^{3+} concentration of less than 10%, the absorption coefficients are low ($\sim 31\text{cm}^{-1}$ in 5%



PRIMARY FOCUSING LENS



OPTION: SPATIAL FILTER

04110-23

FIGURE 3-1

Tm:YLF at 353.2nm), therefore the absorbed energy in a transverse slab can only be ~31%, per cm in length, of that in a longitudinally pumped crystal. This is because, for exponentially absorbed beams the deposited energy E_D is

$$E_D = -\frac{\partial E}{\partial L} = \frac{-\partial E_0 e^{-\alpha L}}{\partial L} = \frac{-E_0 \partial e^{-\alpha L}}{L} = +\alpha e^{-\alpha L} E_0 = +\alpha E$$

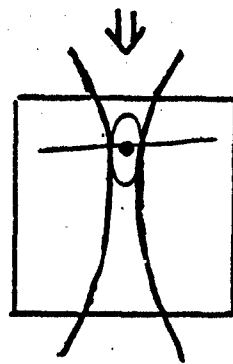
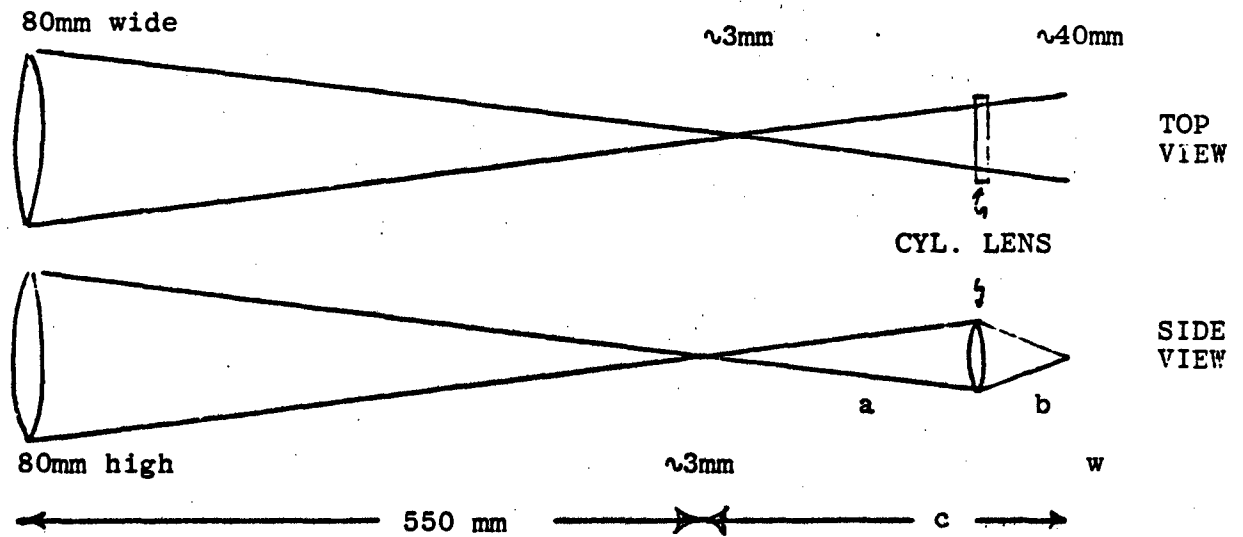
In principle, therefore, one can achieve unlimited energy deposition by making the crystal, and the pump pulse footprint, longer. With fixed energy, however, this translates to making a longer and thinner line focus. As the line gets thinner, its $f/\#$ drops as does the depth of focus. In this manner, as the energy deposited on axis increases, the pumped region shrinks. The amount of energy deposited in the highly pumped region decreases rapidly.

Figure 3-2 shows such a system, along with a two pass system in which a mirror returns the light that passes through the crystal. Variables in such systems are the dopant concentration, focal length of the cylindrical lens and distance (a) of that lens from the initial focus, chosen so that most of the light is captured and focused at the appropriate distance. For the two pass system, another variable is the thickness of the crystal. Four cases are delineated on Table 3-1.

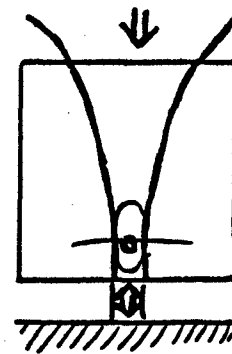
While such systems are capable of very high ($>30\text{J}/\text{cm}^2$) energy depositions, two problems are seen. Firstly, the excited regions are very narrow in these cases, about one to two millimeters across. It is quite difficult to align the axis of a resonator to such a thin plane in space. Secondly, almost no energy is absorbed near this axis, even though the calculation included a 2:1 aspect ratio volume. (The height being twice the spot width.)

A method of overcoming these two defects is space filling, multi-pass pumping. Generally these are polyhedral prisms, whose

SIMPLE TRANSVERSE PUMPING



One Pass



Two Pass

FIGURE 3-2

TABLE 3-1

TRANSVERSE PUMPED DESIGN PARAMETERS

Focal Length (f) (mm)	38.5		48.1	
Distance from Focus (a) (mm)	170.2	49.8	148.9	71.1
Magnification	.29	3.42	.48	2.09
Energy Capture	~85%	100%	~95%	100%
One Pass Energy Deposition (J/cm ²)	20.7	2.1	14.6	3.4
Two Pass Energy Deposition (J/cm ²)	30.5	3.0	21.5	5.5
Energy in Central Region: (J)				
One Pass	.32		.60	
Two Pass	.45		.84	
Line Width (mm)	~0.9	~10.3	~1.4	~6.3

5% Tm:YLF

10mm Thick

220mm total distance (c) for 40mm length

7J available at Cyclinder Lens

reflective faces return the unabsorbed light for another pass through the crystal. Trial and error, in sketches, has shown pentagons to be a good compromise between the number of passes, size of the faces and deposition uniformity. Figure 3-3 shows both a regular and an irregular pentagon.

In comparison, the irregular pentagon is clearly superior. The input is at right angles (vs 63°) to the face, the angles are either 90° or 120° (vs 108°), and the entrance face is wider. The regular pentagon does have two advantages, though. It has no small facets plus the light that escapes does so at an angle from the input. This allows the use of a mirror to reintroduce this light into the crystal.

Figure 3-5 (A & B) shows seven equal area pentagons. The first six are the zero through fifth order irregular while the seventh is the regular pentagon. The order refers to the number of unit lengths in the side or

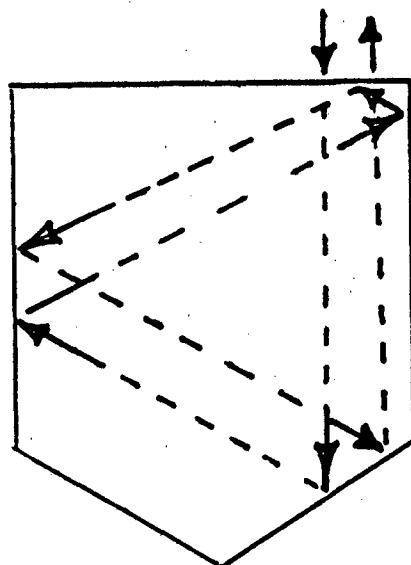
$$N = S / \left(\frac{1}{2} N \frac{1}{\cos 30^\circ} \right).$$

All of the diagrams and accompanying data are based on crystals of 1 unit square area.

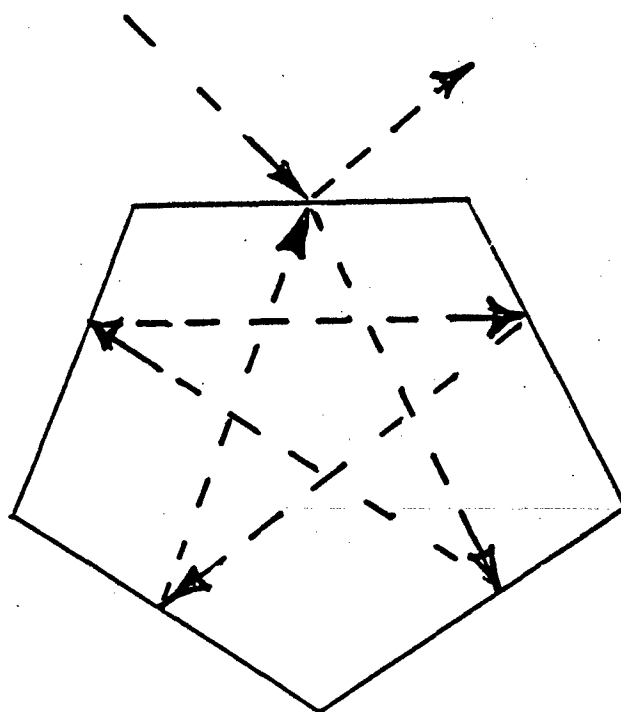
A comparative calculation has been done using a 0.4cm^2 crystal as an example. The energy deposited, and energy stored after $0.15\mu\text{sec}$ for four orders of irregular pentagons and four different dopings were calculated. The answers are expressed as fractions of the input energy. The results are listed in Table 3-2.

The first delay time of zero microseconds gives the total energy deposited. The second delay of $0.15\mu\text{sec}$ corresponds to roughly half the turn on time of the laser, which is the average time the ions spend in the upper manifold.

PENTAGONAL CRYSTALS



Irregular
(order $\frac{N}{n} = 3$)

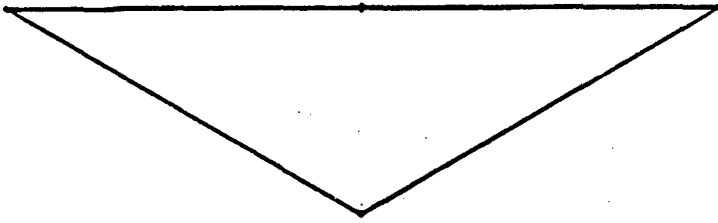
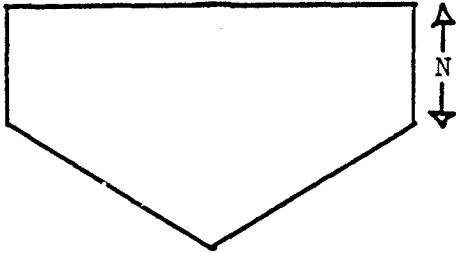
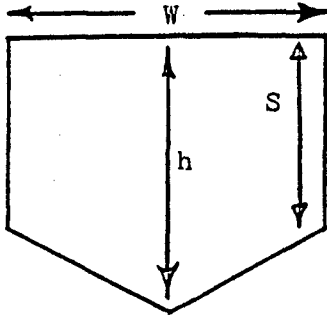
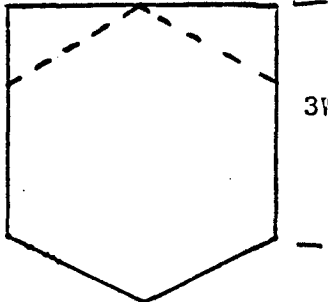


Regular

FIGURE 3-3

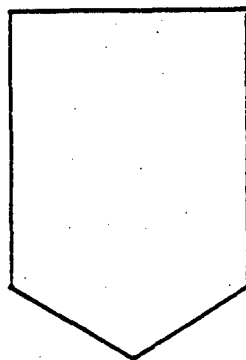
IRREGULAR PENTAGONS

Different Order Solutions for Constant Cross Sectional Area

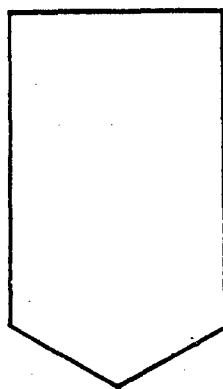
	N	W	S	h	1*
	0	2.63	0	.76	2.28
		.75			
	1	1.52	.44	.88	3.95
		.92			
	2	1.18	.68	1.02	5.10
		.95			
	3	.99	.86	1.15	6.0
		.96			

*1 represents the total path length of the pump beam

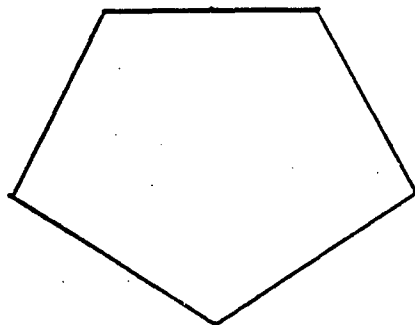
FIGURE 3-4A



N	W	S	h	l*
4	.88	1.01	1.27	6.84
	.97			



5	.79	1.15	1.37	7.56
	.98			



R	.76	-	1.17	5.97
	.87			

*1 represents the total path of the pump beam

FIGURE 3-4B

TABLE 3-2

FRACTION OF INPUT ENERGY DEPOSITED
IN IRREGULAR PENTAGONS

Concentration	Delay (μ s)	<u>Pentagon Order</u>			
		2	3	4	5
3%	0	.37	.41	.44	.45
3%	0.15	.36	.38	.43	.44
5%	0	.53	.57	.59	.61
5%	0.15	.51	.54	.56	.58
7%	0	.64	.68	.70	.71
7%	0.15	.60	.63	.65	.66
10%	0	.75	.78	.80	.81
10%	0.15	.65	.67	.69	.69

We see that there is a monotonic increase in deposited energy as one goes to higher orders and higher dopants, but limits are being approached. Because of the increasing difficulty in fabricating high order solutions, which tend toward a knife blade shape, the optimum is not at any extreme point. This optimum is probably around order 3-4 in 5-7% Tm:YLF.

Table 3-3 lists the stored energies after 0.15 sec for eight solutions: 0.25 and 0.40 cm², third and fourth order solutions and 5% and 7% Tm:YLF. These are calculated using aluminum reflectors of 90% reflectance. Note that although the stored energy density increases as the crystal size decreases, the small faces of the 0.25cm² crystals are ~2.5mm wide. This is near the limit on fabrication of 40mm long crystals. Even at this size, the fluence on the first reflectors is near 3J/cm². This is too much to subject a dichroic coating to, and questionable for bare aluminum.

Finally, we note that these design exercises, while instructive, make implicit assumptions about the pump beam. Prior to a detailed experimental design it was necessary to experimentally determine the pump beam parameters.

Table 3-3

STORED ENERGY*

Crystal Length = 4 cm

Area (cm ²)	Concentration (%)	Order (N)	Energy (J/cm ²)
.25	5	3	12.9
		4	13.7
	7	3	14.1
		4	16.2
.40	5	3	8.2
		4	8.5
	7	3	9.0
		4	9.3

* Delay 0.15 μ s, 7 Joules Input

3.3 INITIAL EXPERIMENTS

Experiments at AERL were carried out in a 3 week period of July 1980. The objectives were:

- (a) Accurate beam profiling of the XeF pump laser.
- (b) Damage testing of Tm:YLF samples.
- (c) Preliminary oscillator experiments.

3.3.1 BEAM PROFILING

In order to design meaningful experiments the intensity variation of the pump laser in the image plane had to be measured. A multiple film plate camera was built to take "photos" of different planes near the focal plane. This device is shown in Figure 3-5. The patterns observed were highly irregular and variable. This showed that the difficulty of quantitatively reducing the exposures to deposited fluence maps was higher than thought, in fact, so much higher that it was beyond the limit of allowable time. Furthermore, the variability of the patterns says that even if such a reduction was done, its value would be limited. Clearly a more general, quicker and less precise method of measuring the beam pattern was needed.

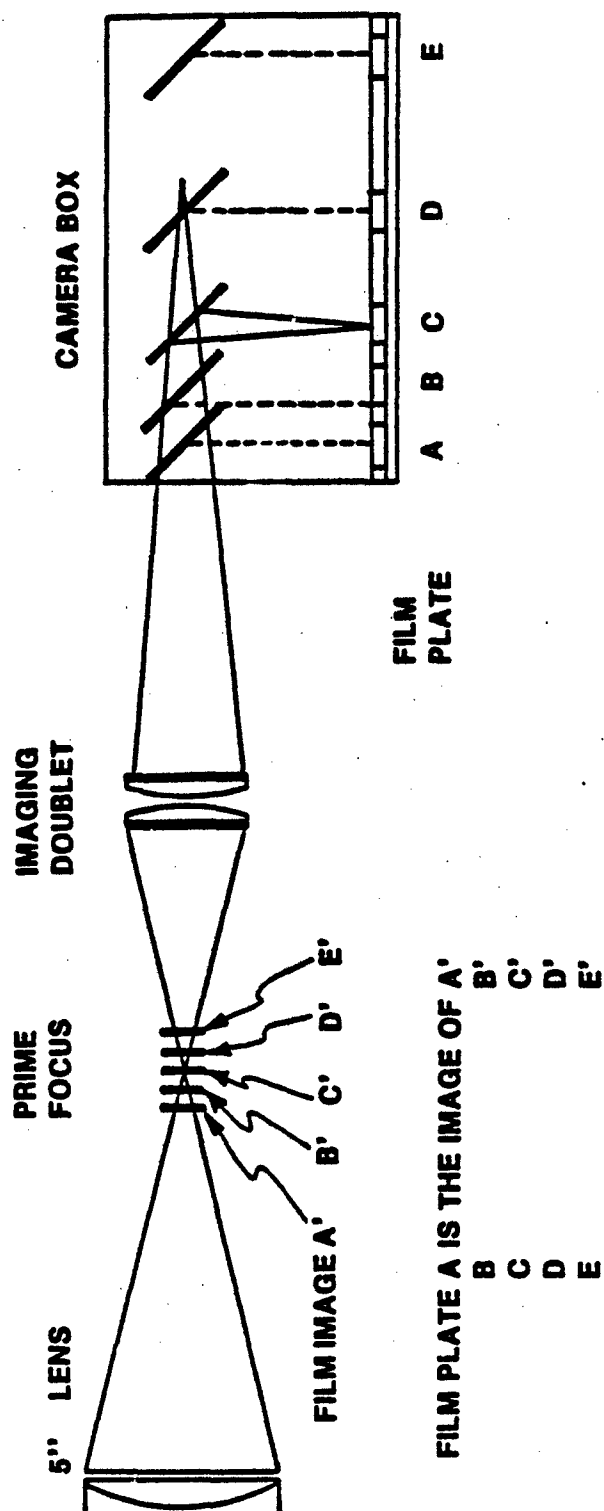
AERL had been using a photosensitive thermoplastic called Lydex to record the beam patterns. This material, which is placed in the beam as in Figure 3-6 and then heat treated in a machine with a heated felt roller, worked well for us. Figure 3-7 shows a series of exposures taken with filters of increasing density at one location.

The intense hot spot in the beam center is the order of 100 X the fluence at the beam edges. Furthermore the hot spot was observed to vary in space from shot to shot. It was clear at this point that the preliminary experimental design would have to be modified drastically.

Defensive Systems Division
Federal Systems Group



PRIME FOCUS PROFILING

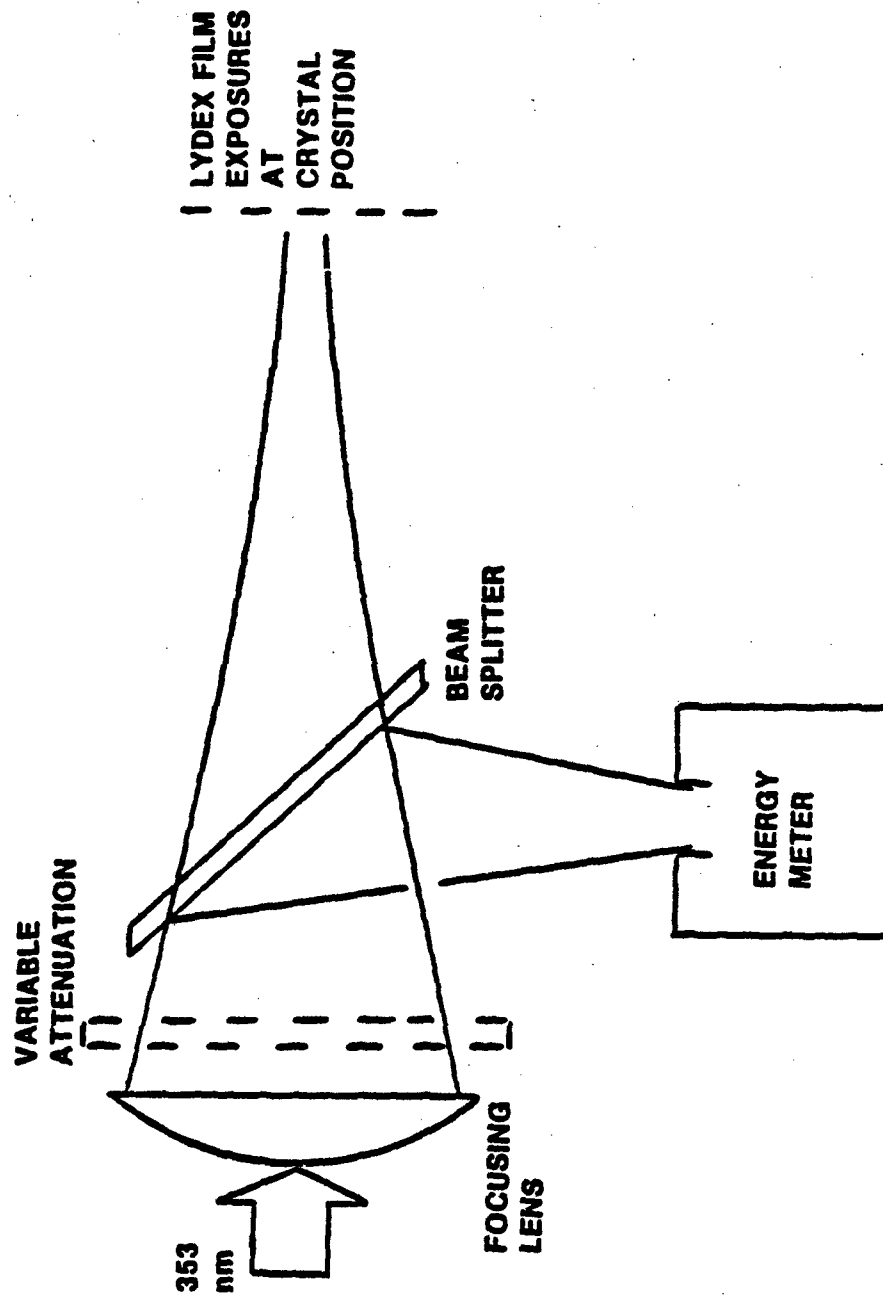


IMAGED PLANES ARE SEPARATED BY 15 MM

Defensive Systems Division
Federal Systems Group



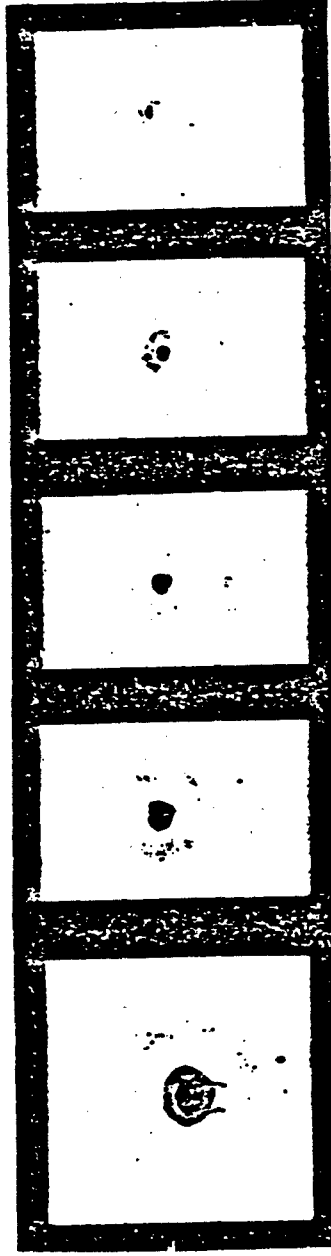
PUMP BEAM PROFILING



Defensive Systems Division
Federal Systems Group



LYDEX EXPOSURES



ENERGY: 8.2J 2.0J 800 mJ 250 mJ 100 mJ

3.3.2 DAMAGE TESTING

Energy calibration was the first step in damage measurements. A monitor calorimeter was placed in position to read energy reflected off a beam splitter located in front of the input oscillator mirror. Another energy meter registered energy which would be incident on the crystal. After consistent calibration was obtained, Tm:YLF crystals were inserted in the oscillator - here the damage measurements were performed.

Initially a 5mm diameter aperture was placed at the crystal face and a fluence of $9.3\text{J}/\text{cm}^2$ caused damage (see Figure 3-8). Previous determination of the damage threshold of YLF at 1.06 and $0.532\mu\text{m}$ had resulted in measured damage fluences $>50\text{J}/\text{cm}^2$ in Q-switched (20ns) pulses. The 1.06 and $.532\mu\text{m}$ data were spatial averages with a multimode laser. The damaging fluences quoted for the XeF laser do not take into account the intense hot spot ($\sim 1\text{mm}$ dia.) in the central part of the focused spot but represent spatial averages over the 5mm aperture. With a 3mm aperture the calculated fluences are considerably higher - measurements were attempted with a 1mm aperture but were invalidated by the plasma formation at the aperture.

3.3.3 OSCILLATOR EXPERIMENTS

The intense hot spots in the focal plane of the pump laser imposed severe problems in the implementation of the oscillator experiments. What is desired is a fairly uniform deposition of the pump fluence on the front face of the crystal with a face fluence of about $30\text{J}/\text{cm}^2$.

It was found that the focus of the XeF beam, which came from a flat-flat resonator, was not only highly irregular, but inconsistent. Shots taken only an hour apart would have totally different patterns and intense hot spots would be formed in unpredictable areas of the

Measured Damage Fluence

XeF Laser**

5mm Aperture

CRYSTAL DESCRIPTION			SURVIVED	DAMAGED
555.15	5% Tm:YLF	Std. Feed, Laser Polished	5.1J cm ⁻²	16.4J cm ⁻²
555.12	5% Tm:YLF	Std. Feed, Laser Polished		9.3J cm ⁻²
558.1	1% Tm:YLF	Std. Feed, Optically Polished	6.7J cm ⁻²	*
312f.15	10% Tm:YLF	Std. Feed, Laser Polished	9.6J cm ⁻²	*
Dichroic Coating			7.0J cm ⁻²	11J cm ⁻²
Dichroic (α)			2.7J cm ⁻²	3.0J cm ⁻²

* Damaged due to laser beam reflecting off crystal wall

3mm Aperture

CRYSTAL	SURVIVED	DAMAGED
555.12	16.4J cm ⁻²	26.9J cm ⁻²
312f.15	22.6J cm ⁻²	24.5J cm ⁻²
Dichroic (α)	2.2J cm ⁻²	3.5J cm ⁻²
Quartz	28.0J cm ⁻²	--

**Pulsewidth

FIGURE 3-8

focal plane. On the other hand, the outer edge of the spot was already larger than the 1cm^2 crystals, so there was no question of using a softer focus to lessen the "hot spot" problem.

Furthermore, the Lydex exposure indicated variations $>100:1$ in intensity from the small central hot spot to the periphery of the imaged spot and the damage tests indicated that the only measurable experiment which could be performed with the equipment and within the time allotted was coupling the central hot spot of the Xef beam

The major difficulty of this approach (coupling of the "hot spot") was that accurate diagnostics were impossible as the deposited fluence in the lasing region could only be crudely estimated.

The oscillator was aligned to the hot spots of the XeF pump via lydex film. From the results of the damage measurements we began pumping at below the assumed damage limit and slowly increased the pump fluence by removing filters to determine threshold for Tm:YLF. A Scientech high-speed photodiode (with narrow-band blue filter) and calorimeter were located on-axis behind the output mirror to determine if lasing occurred. After several shots with no apparent lasing in the blue the calorimeter-photodiode unit was removed in order to set up a screen to photograph the laser while firing. A lite-mike was used for pulse detection scattered off the screen.

On the subsequent shots, laser pulses were detected by the lite-mike and photographs also indicated lasing had occurred. At this point the XeF laser failed thus prohibiting any documentation of the pulse - hence no conversion efficiency values were obtained.

3.4 DESIGN IMPROVEMENT

The highly irregular beam of the lm device necessitated complete redesign of the optical coupling apparatus. These are described below.

3.4.1 OPTICAL INTEGRATORS

Several ways were suggested to form uniform beam patterns from highly non-uniform beams. One which has been used on large CO₂ lasers, was to use many small mirrors, whose reflections overlap in the plane of interest.

While the construction of one of these devices appeared to be uncomfortably difficult and time consuming, it was known that such

devices were stock items, for the far IR, from SPAWR Optical Research. One of these devices was ordered with a custom coating of aluminum to provide good reflectivity at 350nm. It consists of 32 $\frac{1}{2}$ " x $\frac{1}{2}$ " (12.7mm x 12.7mm) mirrors whose reflected images overlap at 25" (635mm). While this does not form a small enough spot, a system was designed in which this spot was imaged at 2:1 by a large lens that captured all 32 beams (see Figure 3-9).. A side effect of this arrangement is that each of the 32 beams is focused in space and forms its own small hot spot. Care was taken to be sure that these would not fall on any surface, such as the dichroic mirror, or in any material, such as the crystal.

3.4.2 TRANSVERSE

Choices were made among the various options of area, length, dopant and aspect ratio of crystal designs for transverse pumping.

The area is a balance between ease of fabrication and alignment and low fluence on the reflectors, all of which favor large areas, and the intensity of deposited energy, which favors a small area. The final conclusion was that 0.45 CM² was near optimum for 5 - 10% Tm:YLF.

The length was similarly balanced between large transverse dimensions for low pump fluences which favor long crystals and fabrication difficulties which favor short crystals. The final design was set at 40mm.

The desired dopant follows the same arguments as for the longitudinal crystals, except that the absorption coefficient is of somewhat greater importance. It was felt that two crystals, one of 7% Tm:YLF and one of 10% Tm:YLF would both be useful, in and of themselves and in contrast with each other.

Intermixed with these decisions was the choice of impact ratio.

INTEGRATOR EXPERIMENTAL LAYOUT

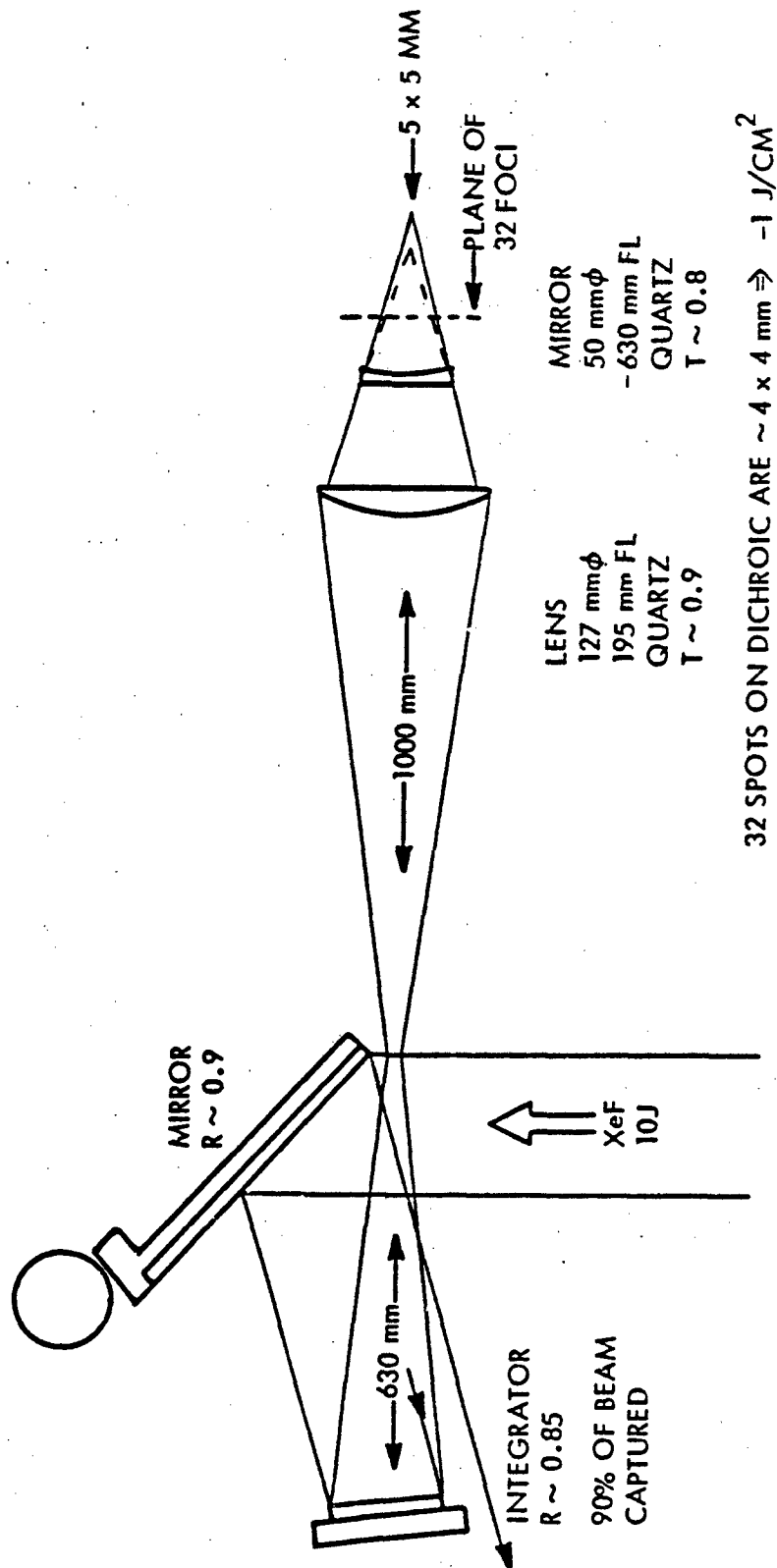


FIGURE 3-9

10150-1

While higher ratios provide longer absorption paths, the 120° faces at the "bottom" become unmanageably thin, and the shape of the whole crystal deviates further and further from a circle (see Figure 3-10). An obvious compromise was N:2 where all the faces except the entrance face are of equal size. This crystal is shown in Figure 3-11 and 3-12.

While there was insufficient time to have crystals fabricated for the upcoming October experiments, the importance of non-imaging pumping, shown by the erratic beam profiles seen in July, led us to order a pair fabricated for the third experiment series. The remaining large stock piece of 10% Tm:YLF and the entire boule of 7% Tm:YLF grown specifically for this purpose, was sent out for fabrication.

To be fabricated with the crystals were two sets of four interchangeable reflector blocks, Figure 3-13. An appropriate holder was made so that any given block could be replaced with any block from the spare set if, for instance, its coating was damaged. These coatings on the bevel side of each block were to have high reflectivity at 353nm and 30° of incidence.

Simple pump optic was designed at this time. It was a variant of the original reimaging pump optics, using a cylinder lens to collapse the small collimated beam to a line. This is shown in Figure 3-14.

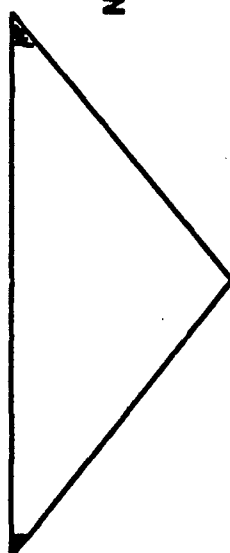
3.5 OCTOBER EXPERIMENTS

3.5.1 EXPERIMENT OBJECTIVES

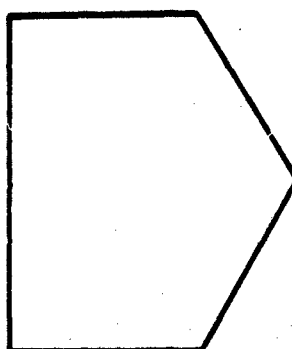
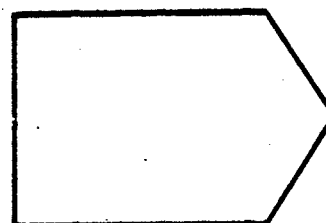
The objectives of the October experiments were to perform diagnostics on the Tm:YLF laser output beam, to determine the conversion efficiency of an XeF pumped Tm:YLF oscillator and to test the alternate coupling optics efficacy in producing uniform spots from the highly nonuniform XeF beam.

 **SANDERS**
Industrial Systems Group

EQUAL AREA PENTAGONS



**O
=
N**


$$\mathbb{N} = \mathbb{Z}$$


11
 22
 33



N = 50

06221-14

FIGURE 3-10

Defensive Systems Division
Federal Systems Group



NEW TRANSVERSE CRYSTAL DESIGN

ORDER N = 2

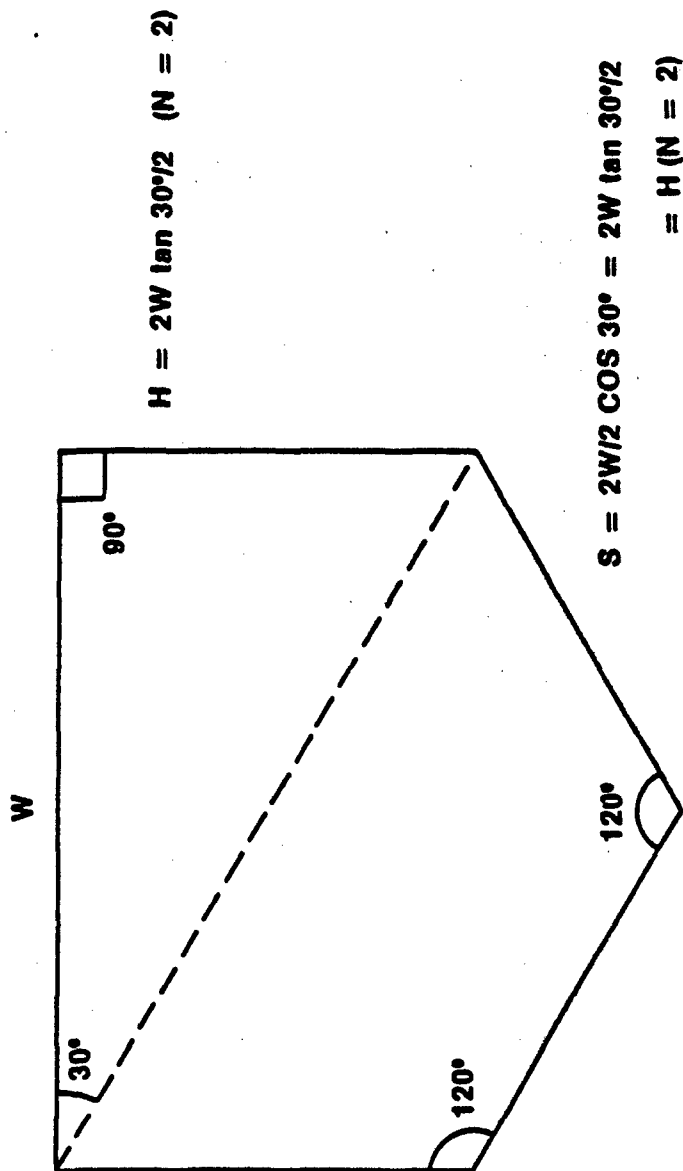


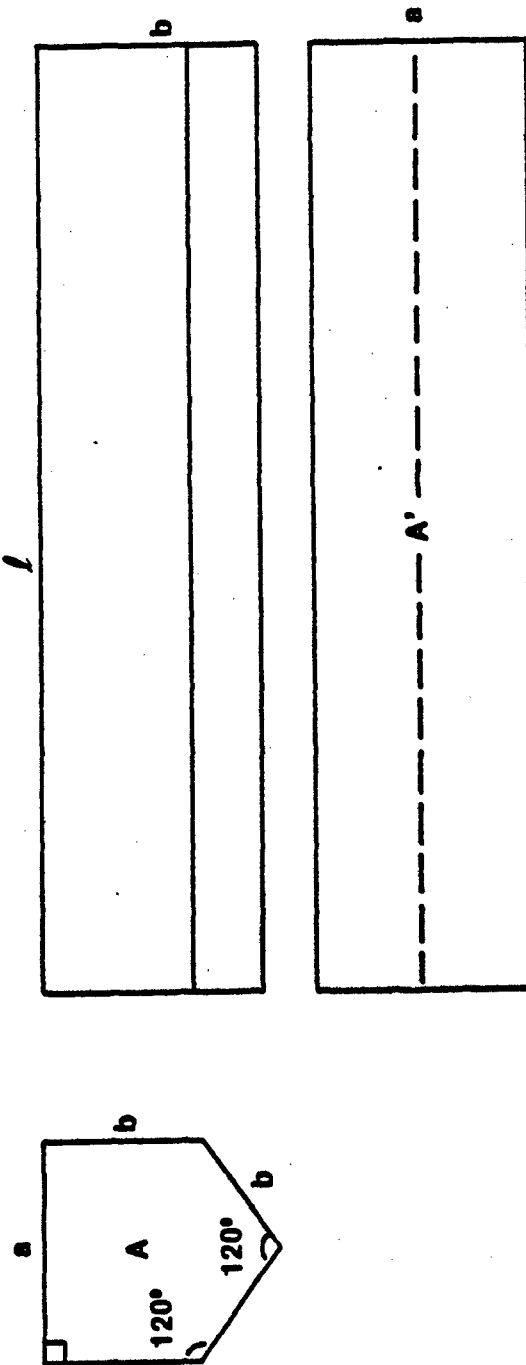
FIGURE 3-11

06221-15

Defensive Systems Division
Federal Systems Group



A 0.45 CM² TRANSVERSE PUMPING CRYSTAL



$A = .45 \text{ CM}^2$
 $A' = 3.16 \text{ CM}^2$

$a = 7.9 \text{ mm}$
 $b = 4.6 \text{ mm}$
 $l = 40. \text{ mm}$

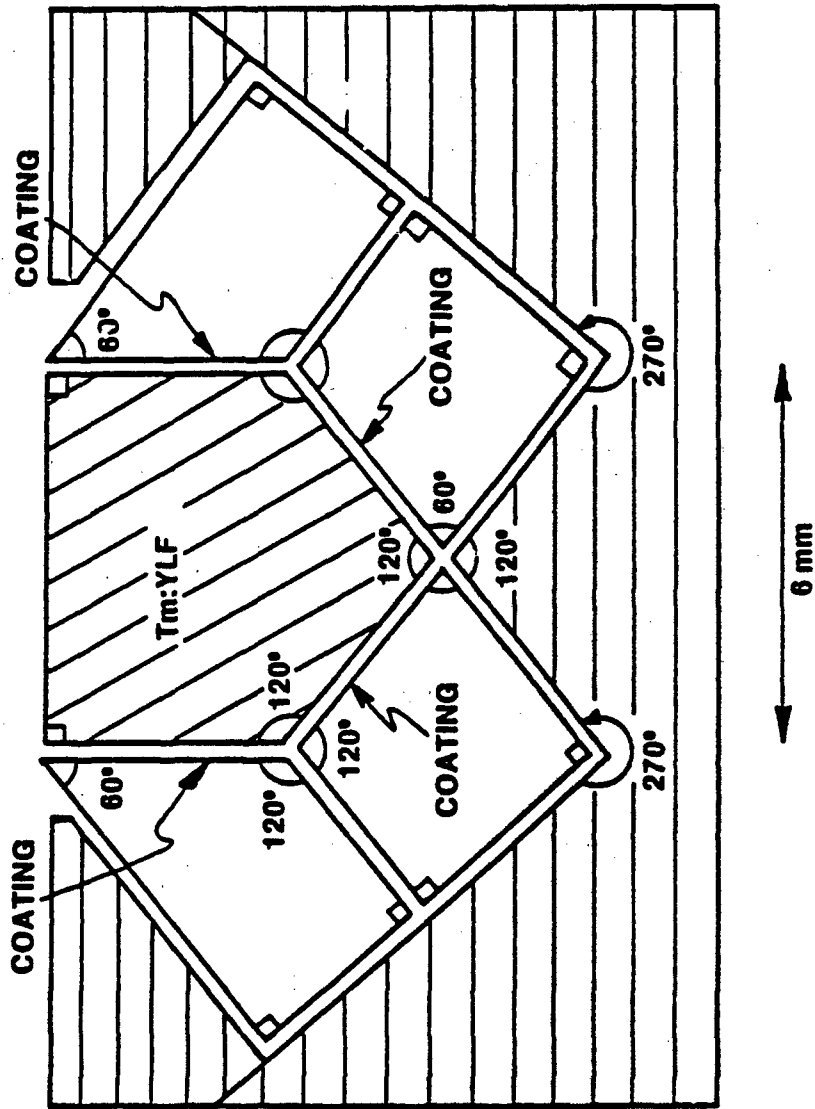
7 J In	5.5 J ABSORBED	12 J/CM ²	7% Tm:YFL
	6.2 J ABSORBED	14 J/CM ²	10% Tm:YLF

Defensive Systems Division
Federal Systems Group



SANDERS

TRANSVERSE PUMPING ASSEMBLY WITH EXTERNAL REFLECTORS



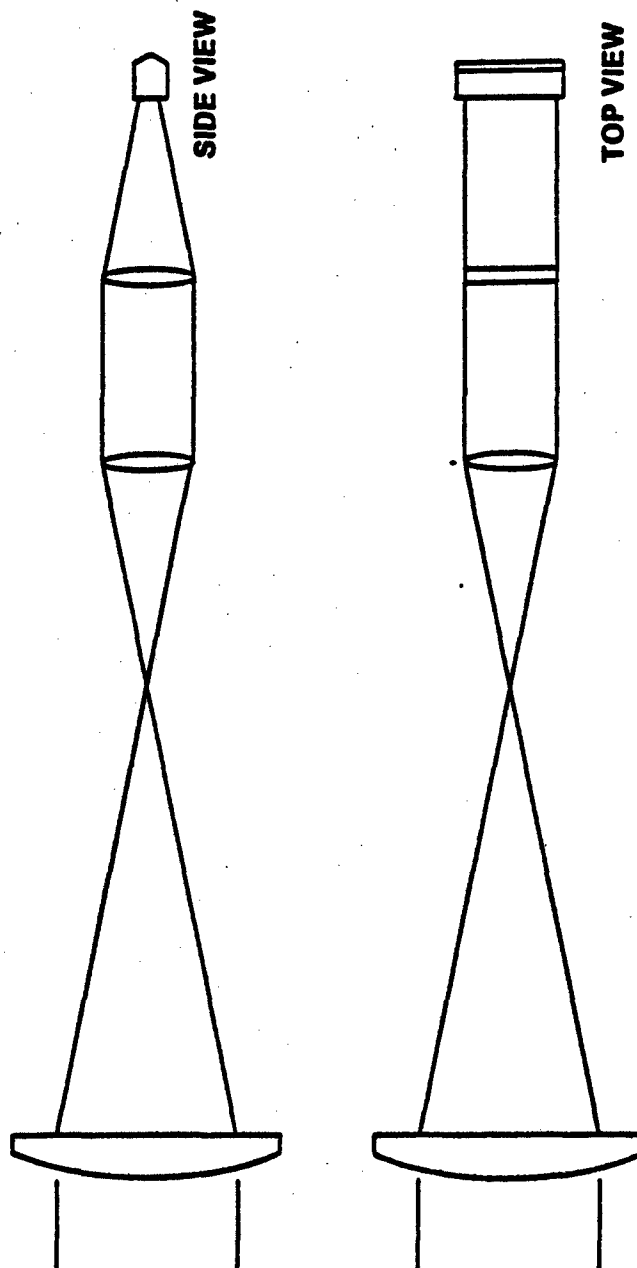
06221-12

FIGURE 3-13

Defensive Systems Division
Federal Systems Group



TRANSVERSE RELAY OPTICS



06221-4

FIGURE 3-14

3.5.2 OSCILLATOR EXPERIMENTS - DIAGNOSTICS

The oscillator geometry and instrumentation to resonantly pump Tm:YLF is shown in Figure 3-15. After aligning optics and 5% Tm:YLF crystal (10 x 10 x 60mm) to the central hot portion of the XeF pump lasing occurred on subsequent shots. The 450nm oscillator output was π polarized, with a pulsewidth of 100ns (see Figure 3-16). Energy output of 50mj in the blue was measured.

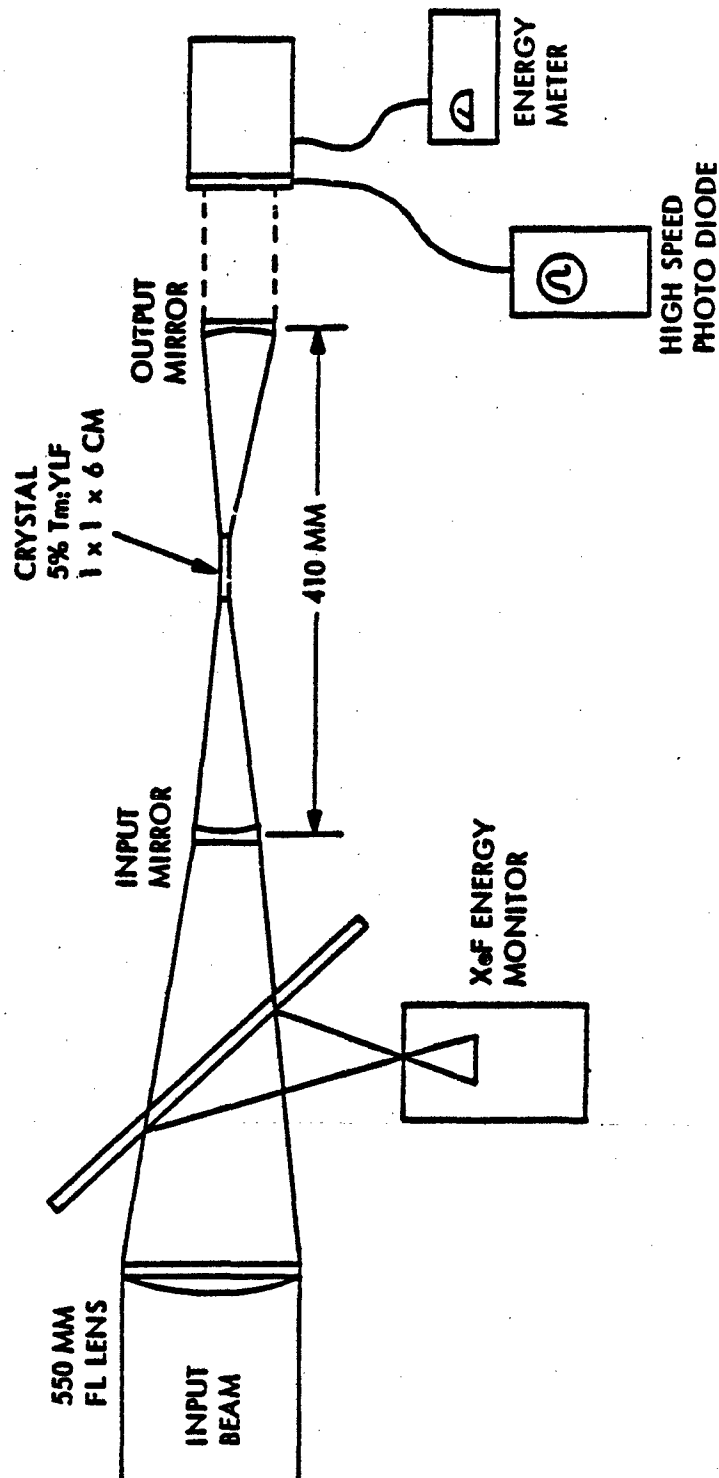
Beam diagnostics were carried out by reflecting the blue light to the screen cage. This enabled the operation of the high speed detectors out of the EMI environment of the XeF laser.

The polarization of the output was found by placing a polarizer in front of the "lite-mike" detector which also has a 450nm narrow band filter over the active area. The polarizer was rotated 90° between subsequent shots. At the same time, the test was done visually, with a polarizer in the opposite orientation. Most shots indicated transmission with the polarizers π oriented; none transmitted with σ orientation. The beam path was checked to insure that none of the reflections rotated the polarization between the crystal and the detectors.

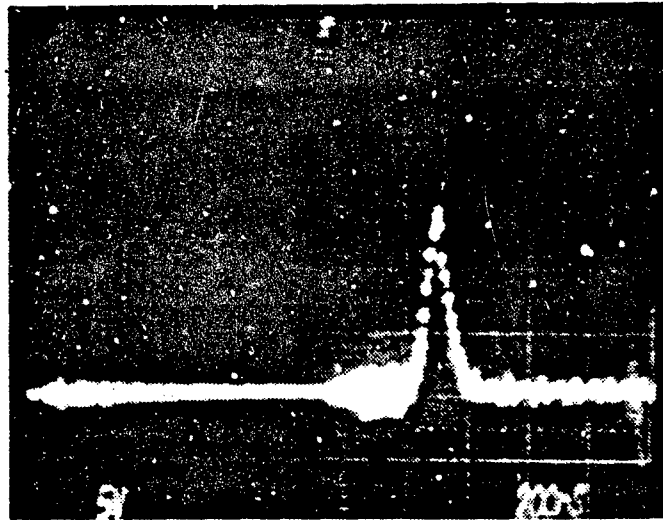
The pulsewidth and relative timing were recorded in each of the polarization checks where the polarizer transmitted. One trace of the output pulse is shown in Figure 3-16, as is an XeF pulse, both on a much expanded scale. The traces have the same time scale and starting time.

The output energy was detected by a Scientec 1" volume absorbing calorimeter, located directly outside of the resonator, with a narrow band 450nm interference filter covering the aperture. Compensating for the transmission of the filter, the largest recorded output was 50mj. This was for a shot where 5J of 353nm light was incident on the crystal. Seventy percent of this energy was absorbed

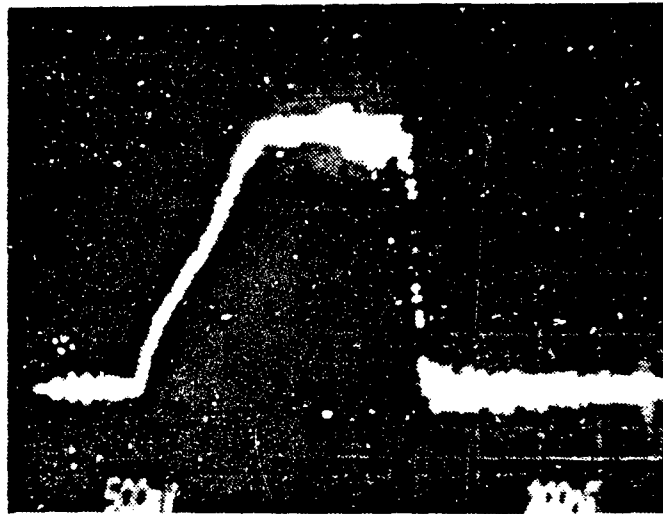
OSCILLATOR EXPERIMENT, WITH DIAGNOSTICS



INPUT/OUTPUT LASER PULSES



450 NM OUTPUT PULSE



353 NM PUMP LASER

FIGURE 3-16

by the crystal. Although precise measurements of the energy deposition profile are impossible because of its variability and gross irregularity, observation of several Lydex exposures, taken in the region occupied by the crystal, led to an estimate that 30% of the pump energy was within the active region. Therefore, approximately 1.0J was deposited in the lasing volume, so the calculated conversion efficiency is 5%.

3.5.3 INTEGRATOR TEST

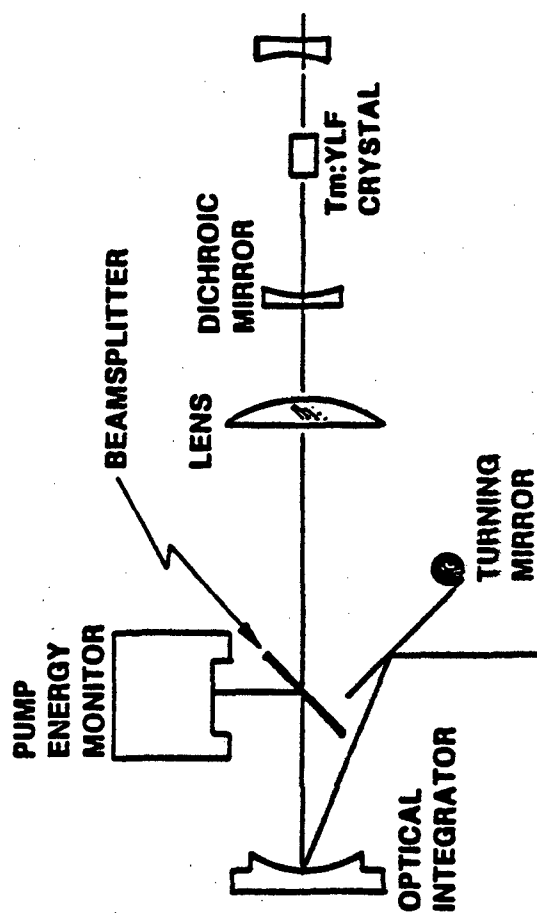
The oscillator experiment, shown in Figure 3-17 was set up on the last day of experiments at AVCO using a 240mm focal length lens from our lab.

A Lydex exposure was made of the first "focus" of the integrator. Figure 3-18 compares the pattern to one taken of a focused spot. If one looks at the original, the extreme uniformity of the integrated spot is apparent, as is the extreme irregularity of the other.

Before the crystal was placed in the oscillator, a throughput measurement was taken for 9.6J of pump, only 2.2J were passed through the dichroic mirror. It was not known where the energy was being lost, as the expected delivered energy was ~6J.

With this low throughput, it was not surprising that the oscillator did not lase. However, the usefulness of the integrator, in forming small uniform pump regions, was demonstrated.

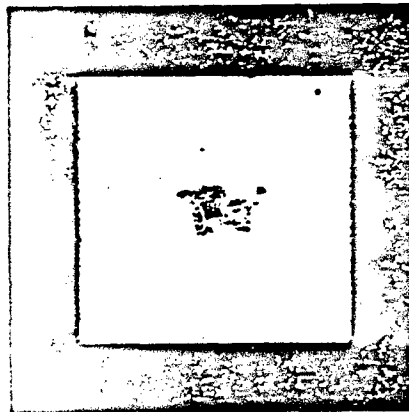
INTEGRATOR EXPERIMENTS



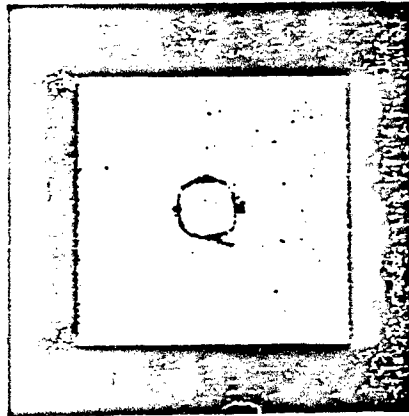
Defensive Systems Division
Federal Systems Group



BEAM CROSS-SECTION COMPARISON



QUARTZ LENS



OPTICAL INTEGRATOR

FIGURE 3-18

06051-18

3.6 AMPLIFIER MEASUREMENTS

The experience of the first two experimental sections led to a complete redesign of the experiments for the final session at AERL. The reasoning is simple:

In the initial experimental design and modelling a longitudinally pumped oscillator with a plane wave input was assumed. Oscillator experiments, although conceptually simple, require rather high pump fluences to obtain sufficiently high gain for efficient extraction. For example, typical values of \bar{g}_0 for a resonant pumped system⁽³⁾ operating with good (40%) efficiency is 0.4 cm^{-1} . In order to obtain an average gain coefficient of 0.2 cm^{-1} in Tm:YLF, a pump fluence of $\sim 30 \text{ J/cm}^2$ is needed. This would be straightforward with a clean pump beam; but the focal plane fluence measured in the preliminary experiments at AERL exhibited variations of $>100:1$. With the beam integrator reasonably uniform "focal plane" fluences were obtained at only 10 J/cm^2 which provides a corresponding gain coefficient of 0.08 cm^{-1} - a gain too low for efficient oscillator operation.

A further requirement for efficient oscillator operation is precise alignment of the crystal with the resonator mirrors and with the pump beam. This was a particularly difficult aspect of the experiments at AERL as the XeF laser was erratic and the hot spot was not fixed spatially.

The experimental set-up for amplifier extraction is more complex. In addition to the XeF pump optics, a source of extracting energy temporally, spectrally, and spatially matched to the gain medium is required. In spite of this added complexity amplifier measurements appeared more likely to succeed under the constraints of the existing experimental conditions for the following reasons:

(a) High Energy Storage

Full absorption of the pump laser energy in a longitudinally pumped crystal is straightforward. A 5% Tm:YLF crystal of 5 cm length will absorb 80% of the pump laser in a single pass.

(b) Ease of Extraction

The saturation fluence for Tm:YLF is:

$$E_{\text{sat}} = 10\text{J/cm}^2$$

and would be provided by a commercial dye laser which can provide a much "cleaner" beam than the AERL XeF laser.

(c) The stored energy in a Tm:YLF amplifier is very high at low XeF pump fluences - 5J/cm^2 deposited produces $\sim 0.6\text{J/cm}^3$ stored.

(d) Resonant pumped amplifiers are simple to model and subject to far less experimental ambiguity as amplifiers are far less sensitive to precise alignment and to losses.

3.7 FEBRUARY EXPERIMENTS

A final series of experiments, scheduled for six weeks, began February 18. The main goals were to confirm our spectroscopic knowledge and generate significant amounts of blue light using the integrator pumped dye laser seeded amplifier.

3.7.1 SET-UP

Before the excimer laser could be used, some rebuilding work was directed by AERL. Beginning on February 18, Sanders' scientists and an AVCO technician:

- Installed new storage capacitors
- Repaired the Marx bank erecting spark gaps

- Repaired the E-gun feedthrough bushings
- Rewired the electrical components
- Filtered the insulating oil and refilled the high voltage section
- Installed new laser mirrors
- Removed, cleaned and replaced the gas cell windows

While this was going on, the dye seeded amplifier experiment was being constructed. The set-up is diagrammed in Figure 3-19 and the layout in the laboratory shown in Figure 3-20.

Timing of the pump (XeF) and extracting (dye laser) beams was effected by splitting a fraction of the pump and extracting beams to a photodiode in the screen cage.

A removable mirror directed the blue beam to a polychromator/OMA which was used to measure its wavelength. By illuminating a crystal of Tm:YLF with filtered output from a Xenon arc lamp polarized fluorescent spectra were obtained. By noting the center channel on the display oscilloscope, hooked to an optical multi-channel analyzer, the dye laser was tuned to the same wavelength.

3.7.2 FIRST SESSION WITH THE XeF LASER

The XeF laser was first run on March 6. The output, measured at the output mirror, was 7 Joules. The relative pulse timing was established, with the dye laser following the XeF laser by about $\frac{1}{2}$ μ sec.

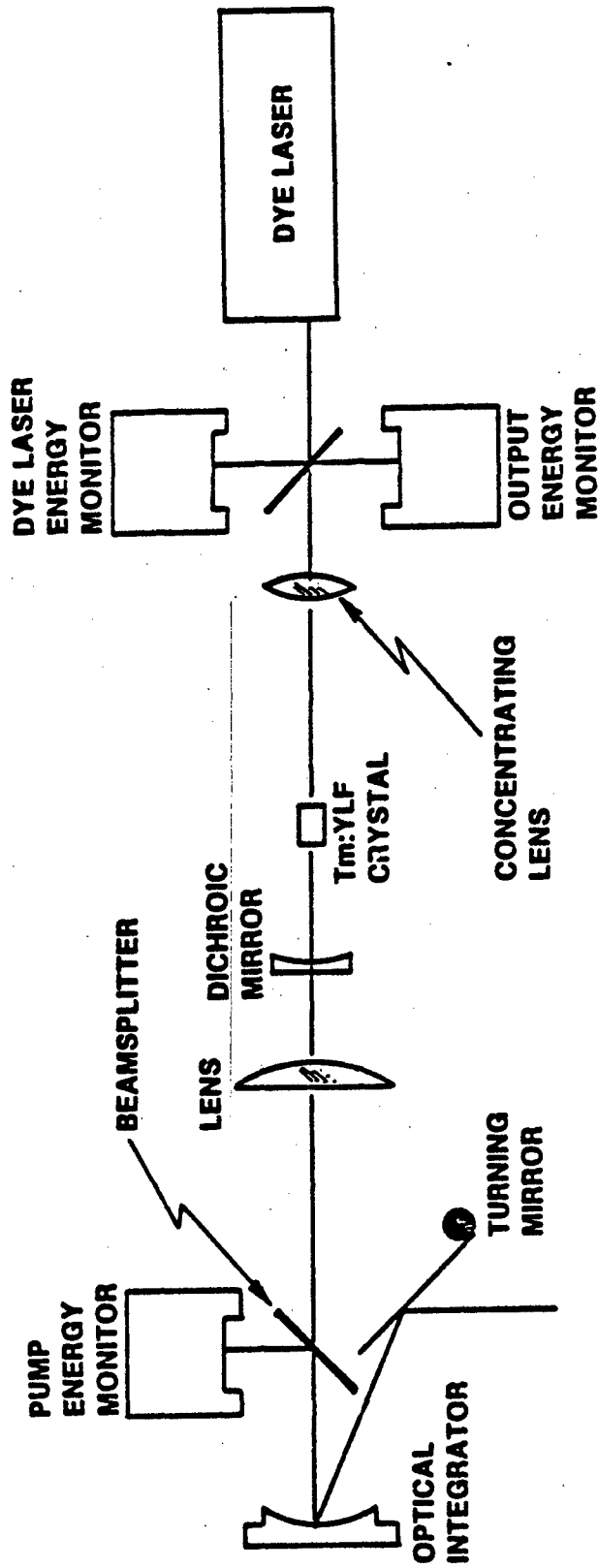
The XeF beam was walked through the experiment optics, off the flat tuning mirror, to the optical integrator and through the relay lens.

Beam profiles were established by taking sequential exposures down the axis. For collinearity, a piece of Lydex was taped to the back of a piece of exposed film, and placed where the crystal would

Defensive Systems Division
Federal Systems Group



INTEGRATOR EXPERIMENTS



Defensive Systems Division
Federal Systems Group



AMPLIFIER EXPERIMENT AERL FLOOR PLAN JUN - APR 1981

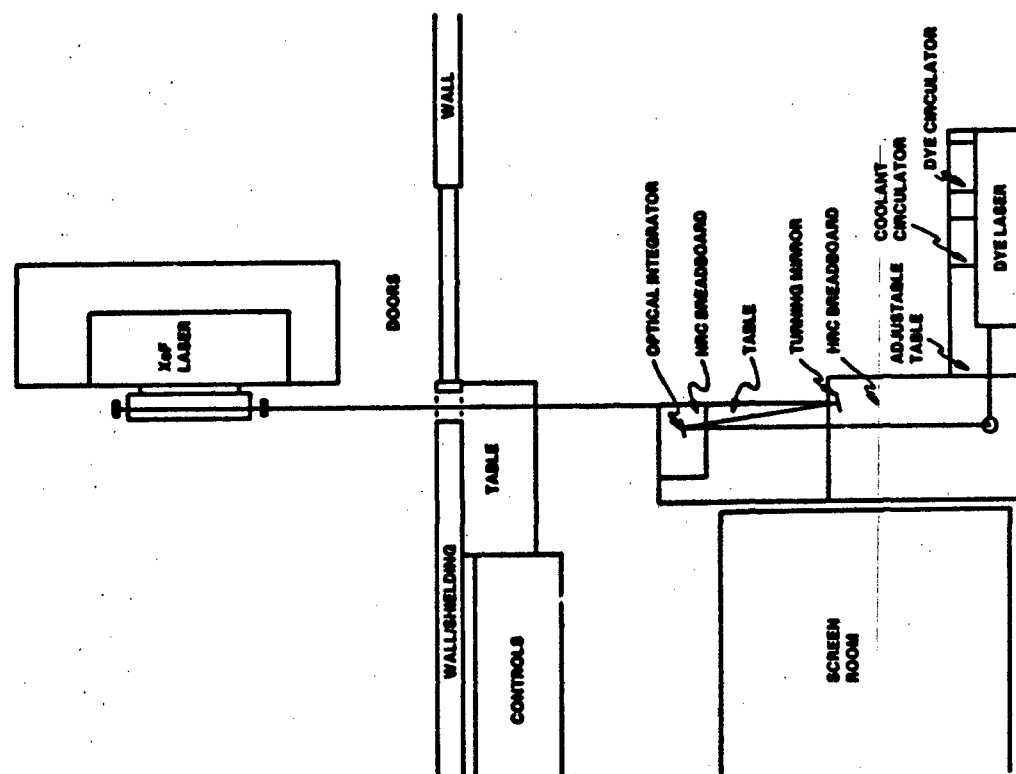


FIGURE 3-20

06221-5

go. The dye laser beam burnt the film emulsion and the XeF beam exposed the Lydex.

By holding this to the light, it was seen that the dye laser beam was fit perfectly within the square spot of the XeF beam.

The energy monitoring meters were calibrated using the 4" Scientech. At this point, for each shot the XeF energy and the pulse-width and relative timing of the two beams was measured. The dye laser was so consistent that to obtain its energy, two shots were taken, one during the XeF shot and one afterwards.

At this point, of 7 Joules of XeF energy coming out of the XeF laser only a 1 - 1.5J were incident on the crystal face. Most of the rest is lost due to the geometry, the size of the optics and the divergence of the XeF laser.

Beginning March 17 crystals were put in the beams and measurements were taken of the fraction of the blue beam after the crystal, both with and without firing the XeF laser. Those combinations tried were:

10% Tm:YLF	452.6 nm σ
10% Tm:YLF	452.7 nm π
10% Tm:YLF	452.6 \pm 1.5 nm σ
5% Tm:YLF	452.6 nm σ
7% Tm:YLF	448.5 nm π

No gain was ever conclusively recorded. Although there was only 1J incident on the crystal, some gain should have been seen just above the noise.

An obvious possibility for error would be wavelength error. After discussing the problem, it was agreed that the dye laser line was narrow and stable enough for the experiment but that we needed a more accurate

way of recording the wavelengths. To this end, a diffuser was installed in a fixed position near the Polychrometer entrance slot, and imaged into it. This eliminated the wavelength errors due to angle changes that occurred when focusing the crystal or dye laser directly on the slit.

On March 20 this was put to the test. The 10% crystal was placed on the σ orientation and the dye laser tuned to the 452.6 nm peak. However, the XeF laser had degraded further and only $\frac{1}{2}$ J was being delivered to the crystal. It was not surprising that no gain was measured.

3.7.3 MODIFIED SET-UP

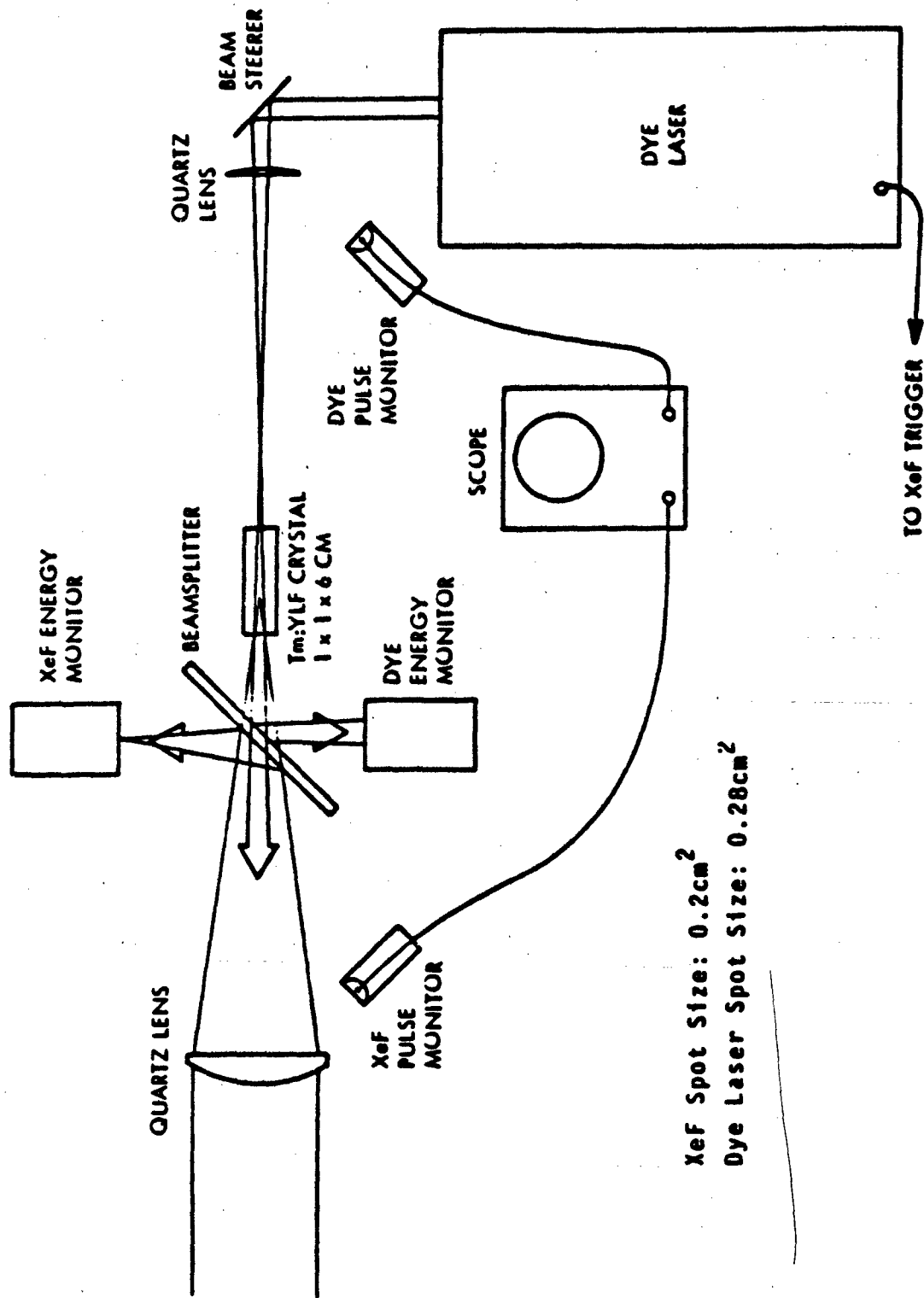
Because of the lack of XeF energy a new experimental design was erected and built. This used a 9.6m radius of curvature turning mirror coated for maximum reflectance at 353nm, supplied by AVCO. This improved the reflectivity over the flat turning mirror and, more importantly, induced the XeF beam size to that of the integrator, thus eliminating spillover.

Unfortunately, as this was being set up, and the XeF beam "walked through" the experiment, both the Marx bank and the foil blew. From March 23 through April 9, the XeF laser was never operable long enough to align the system. The problems included nine blown foils, four blown charging resistors and a non-firing crowbar.

At this time it was reluctantly concluded that the mean time between failures was so short that not enough shots would be generated to align the equipment. Without much enthusiasm, it was agreed that we would resort to a simpler fall-back experiment which required fewer alignment shots (see Figure 3-21). Meanwhile, the XeF laser needed further repairs. In the period of March 14 through 16, a spark gap blew up, the foil was replaced, the cathode repaired and the resistor replaced. By the 17th, our last day at AVCO, the machine was working again.

100 200 300 400 500 600 700 800 900 1000 1100 1200 1300 1400 1500 1600 1700 1800 1900 2000 2100 2200 2300 2400 2500 2600 2700 2800 2900 3000 3100 3200 3300 3400 3500 3600 3700 3800 3900 4000 4100 4200 4300 4400 4500 4600 4700 4800 4900 5000 5100 5200 5300 5400 5500 5600 5700 5800 5900 6000 6100 6200 6300 6400 6500 6600 6700 6800 6900 7000 7100 7200 7300 7400 7500 7600 7700 7800 7900 8000 8100 8200 8300 8400 8500 8600 8700 8800 8900 9000 9100 9200 9300 9400 9500 9600 9700 9800 9900 10000

AMPLIFIER EXPERIMENT



XeF Spot Size: 0.2cm^2
 Dye Laser Spot Size: 0.28cm^2

FIGURE 3-21

3.7.4 FALL-BACK EXPERIMENT

Data was taken in the afternoon and evening of April 17th. The XeF laser operated reliably and between 1 - 3 Joules were delivered to the crystal. Unfortunately, the dye laser output had degraded to 100 - 200mJ and eventually failed, and only 16 data points were obtained.

All the data is shown in Table 3-4. The highest energy extracted, shot #6, was 93mJ. The energy extracted was measured by monitoring with beam splitters the dye laser input and output to the crystal with calibrated photodiodes in each shot. As a check, the blue laser input and output was measured with and without the XeF pump. The temporal delay between pump and extracting pulses was also monitored during each shot.

The intent of these experiments was to extract significant ~ 1 J amounts of blue light. With, for example, 3J of XeF absorbed the stored 452 nm energy is 2.3 Joules and a dye laser fluence of $10\text{J}/\text{cm}^2$, one E_{sat} , would extract about 60% of this, or 1.4 Joules. Unfortunately, during this last attempt the dye laser output dropped to a few hundred mJ and the extracting fluence was less than $1\text{J}/\text{cm}^2$, which for $\text{Tm}^{3+}:\text{YLF}$ is in the small signal gain regime.

DISCUSSION

In spite of the experimental difficulties which prevented the generation of large (~ 1 J) amounts of 452 nm output sufficient data was taken to fit the results to a model of a loss-less $\text{Tm}:\text{YLF}$ amplifier. The major scaling concern for the $\text{Tm}^{3+}:\text{YLF}$ laser is the possibility of ESA (excited state absorption) via the absorption transition:



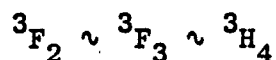
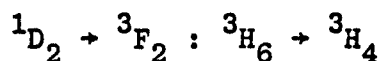
TABLE 3-4

DYE LASER SEEDED - Tm:YLF AMPLIFIER DATA

SHOT #	(nm)	POL	PUMP ENERGY (J)	SEED ENERGY (J)	OUTPUT ENERGY (J)	ENERGY GENER. (mJ)
1	452.7	π	1.6	.134	.168	34
2			1.5	.214	.248	34
3			1.9	.181	.231	50
4			2.3	.208	.228	20
5			1.5	.168	.214	46
6			2.8	.101	.194	93
7			1.2	.221	.235	14
8	452.6	σ	2.1	.161	.161	0
9			3.3	.127	.181	54
10			1.5	.144	.168	24
11	448.5	π	2.5	.161	.181	20
12			1.5	.174	.174	0
13			1.3	.154	.137	X
14			0.6	.154	.154	0
15			1.0	.134	.134	0
16			1.3	.124	.124	0

which is in the vicinity of 450 nm (see Figure 3-22). The absorption spectrum of this transition is not known and is exceedingly difficult to measure; furthermore, the precise position, linewidth and strength of the states within these multiplets are not known to sufficient accuracy to determine whether a loss is present to any of the $^1D_2 - ^3F_4$ transitions. Any such loss would reduce the efficiency of the laser.

The 3H_4 state is, of course, not thermally populated, nor is it pumped directly by the XeF laser. However, at high Tm concentrations the nearly resonant process:



populates 3H_4 . In fact, for each ion initially in 1D_2 , 2 ions are excited to 3H_4 . The rate of this process depends on the Tm^{3+} concentration; this is believed to be the dominant "concentration quenching" mechanism for the 1D_2 state. At low concentration, 1-2%, the relaxation rate of 1D_2 is too slow to significantly populate 3H_4 on the time scale of the generation of laser pulse $\sim 1\mu s$. At higher concentrations the 1D_2 lifetime becomes the order of the time scale of the XeF absorption - Tm:YLF emission and the ESA possibility cannot be excluded. The Tm:YLF amplifier experiment provides a test for the existence of ESA.

MODEL

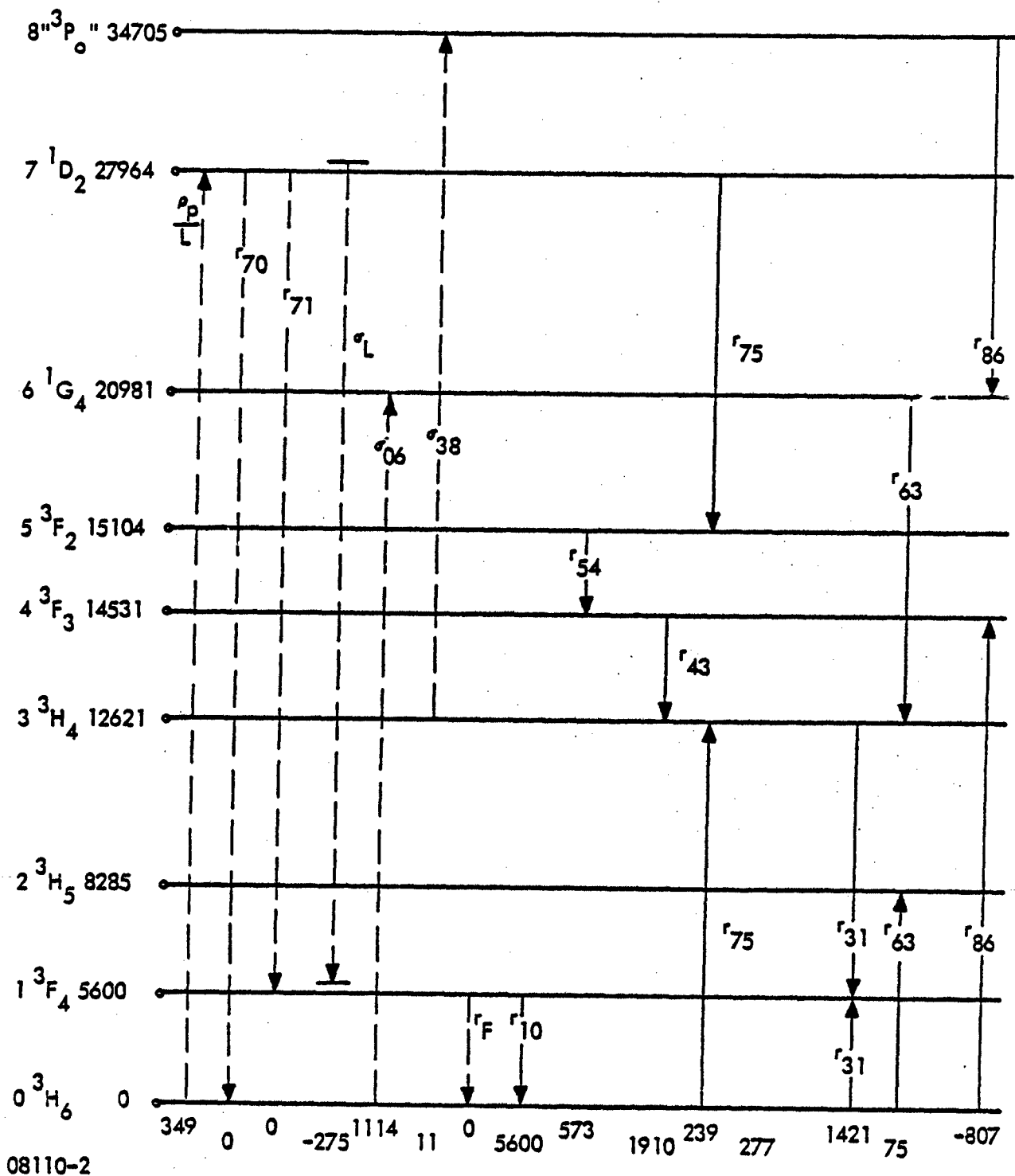
A pump-while-extract amplifier model was developed for the Tm^{3+} :YLF amplifier. If the Tm laser were operated as a true storage laser (lifetime much longer than pump pulsewidth) then the gain is simply:

$$G = \exp (N \cdot \beta \sigma l)$$



Defensive
Systems
Division

LEVELS INVOLVED IN Tm + 3:YLF LASER



08110-2

FIGURE 3-22

when $E_{in} \ll E_{sat}$. However, the Tm^{3+} lifetime in these experiments is the order of the pump pulsewidth so that the storage model is inappropriate. Figures 3-23 and 3-24 illustrate the essential physics of the "pump-while-extract" model, more detail is provided in Appendix A, and a comparison of the predictions and the data is shown in Tables 3-5 and 3-6.

Of the three lines attempted, only the two longer wavelength lines exhibited gain. One possible explanation of this is that the 448.5nm line has a very small linewidth. It is possible that the tuning accuracy, both in the dye laser linewidth and central wavelength stability were insufficient to have good spectral overlap. This is consistent, as both of the other lines are much wider. The 452.7nm line in particular is quite wide, which is why it was attempted first (see Figure 3-25).

Another possibility is that there is some wavelength dependent loss, such as excited state absorption. The definitive test on this, would involve delaying the dye laser pulse by several fluorescent lifetime. This would allow the ions to decay from the upper laser level and populate the intermediate levels, from which an absorption might be originating. Unfortunately, there was no time available for this experiment.

As described in Appendix A, the model uses uniform plane waves, for both pump and seed beams, with top hat profiles. This is a particularly crude approximation of the pump pulse which is an erratic focal volume. Nevertheless, the models produced surprising agreements with the experiments. For the 452.7nm results, excluding the one point with obvious instrument error, the mean error is extremely close to zero, and the standard deviation is less than 50%. There is certainly no evidence here, or at 452.6nm, to indicate any large, unexpected loss mechanism.

Defensive Systems Division
Federal Systems Group



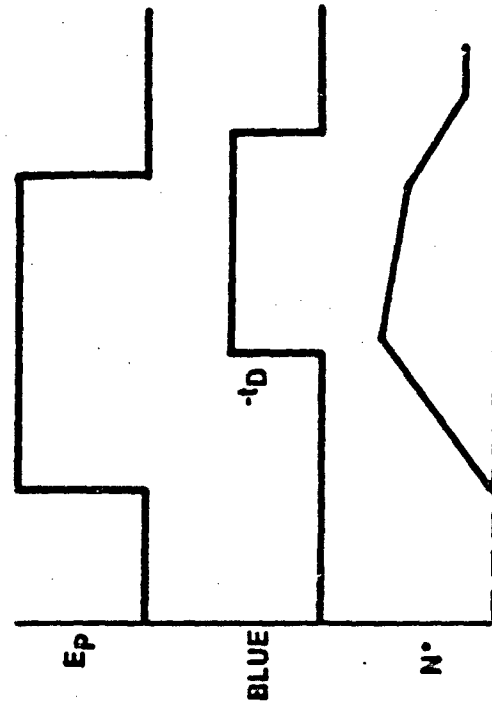
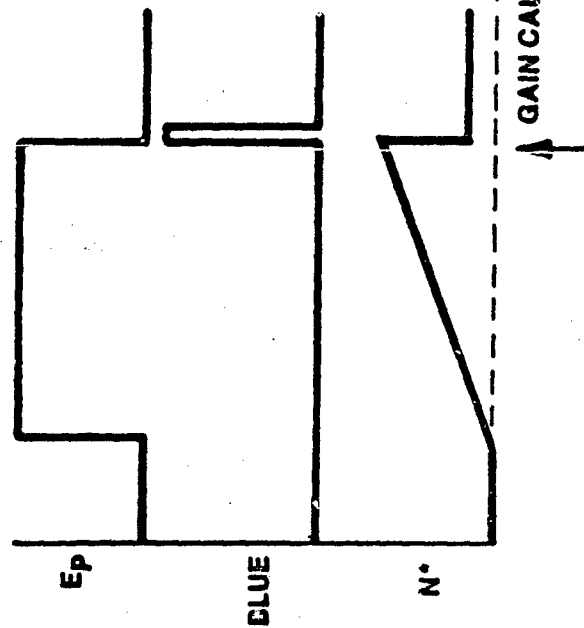
AMPLIFIER MODELS

STORAGE

- N° BUILDS DURING PUMP PULSE
- NO DECAY
- N° EXTRACTED BY BLUE PULSE
- SAT OR SMALL SIGNAL GAIN REGIME

PUMP WHILE EXTRACT

- N° BUILDS IN 1NS BINS
- N° DECREASED BY DECAY AND EXTRACTION IN EACH BIN
- DELAY TIME AND REAL PULSEWIDTHS INPUTED
- SMALL SIGNAL GAIN REGIME



08141-1

Figure 3-23

COMPUTER AMPLIFIER MODEL

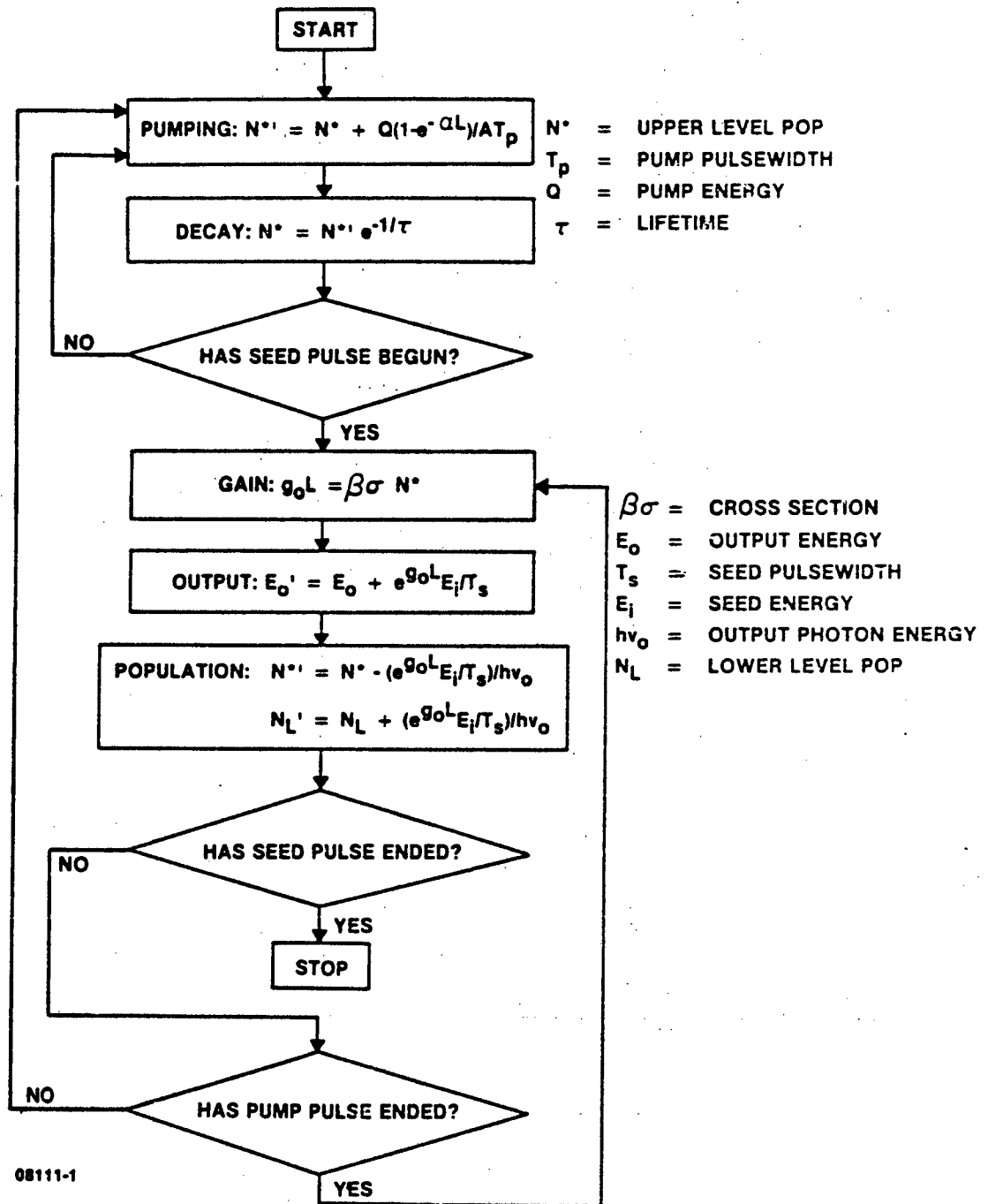


Figure 3-24

Defensive Systems Division
 Federal Systems Group



RESULTS

TABLE 3-5

π LINE 452.7 nm, $\Delta\lambda = 1.2$ nm FWHM

EXEF (J)	STORAGE		MEASURED GAIN	CODE GAIN	BLUE INPUT (mJ)
	$\bar{\theta}_0$ (cm ⁻¹)	$\exp(\theta_0)$			
1.6	0.05	1.35	1.25	1.19	134
1.5	0.05	1.32	1.15	1.17	214
1.9	0.06	1.42	1.28	1.23	181
2.3	0.07	1.53	1.1	1.24	208
1.5	0.05	1.32	1.27	1.18	168
2.8	0.09	1.68	1.92	1.23	101
1.2	0.04	1.25	1.06	1.14	271

Defensive Systems Division
Federal Scientific Group



RESULTS

σ LINE 452.6 nm $\Delta\lambda = 0.8$ nm FWHM
 π LINE 448.5 nm $\Delta\lambda = 0.5$ nm FWHM

TABLE 3-6

	EXEF (J)	STORAGE		MEASURED GAIN	CODE GAIN	BLUE INPUT (mJ)
		\bar{g}_0 (cm ⁻¹)	exp($g_0 l$)			
σ	2.1	0.08	1.65	1.00	1.36	161
	3.3	0.13	2.19	1.43	1.44	127
	1.5	0.06	1.43	1.17	1.24	144
π	2.5	0.13	2.22	1.12	1.44	161
	1.5	0.08	1.62	1.00	1.22	174
	1.3	0.07	1.57	0.89	1.27	154
	0.6	0.03	1.21	1.00	1.12	154
	1.0	0.05	1.38	1.00	1.18	134
	1.3	0.07	1.52	1.00	1.25	124

200 220 240 260 280 300 320 340 360 380 400 420 440 460 480 500 520 540 560 580 600 620 640 660 680 700 720 740 760 780 800 820 840 860 880 900 920 940 960 980 1000

BA  **Defensive
Systems
Division**

TM:YLF ¹D₂ CROSS SECTION

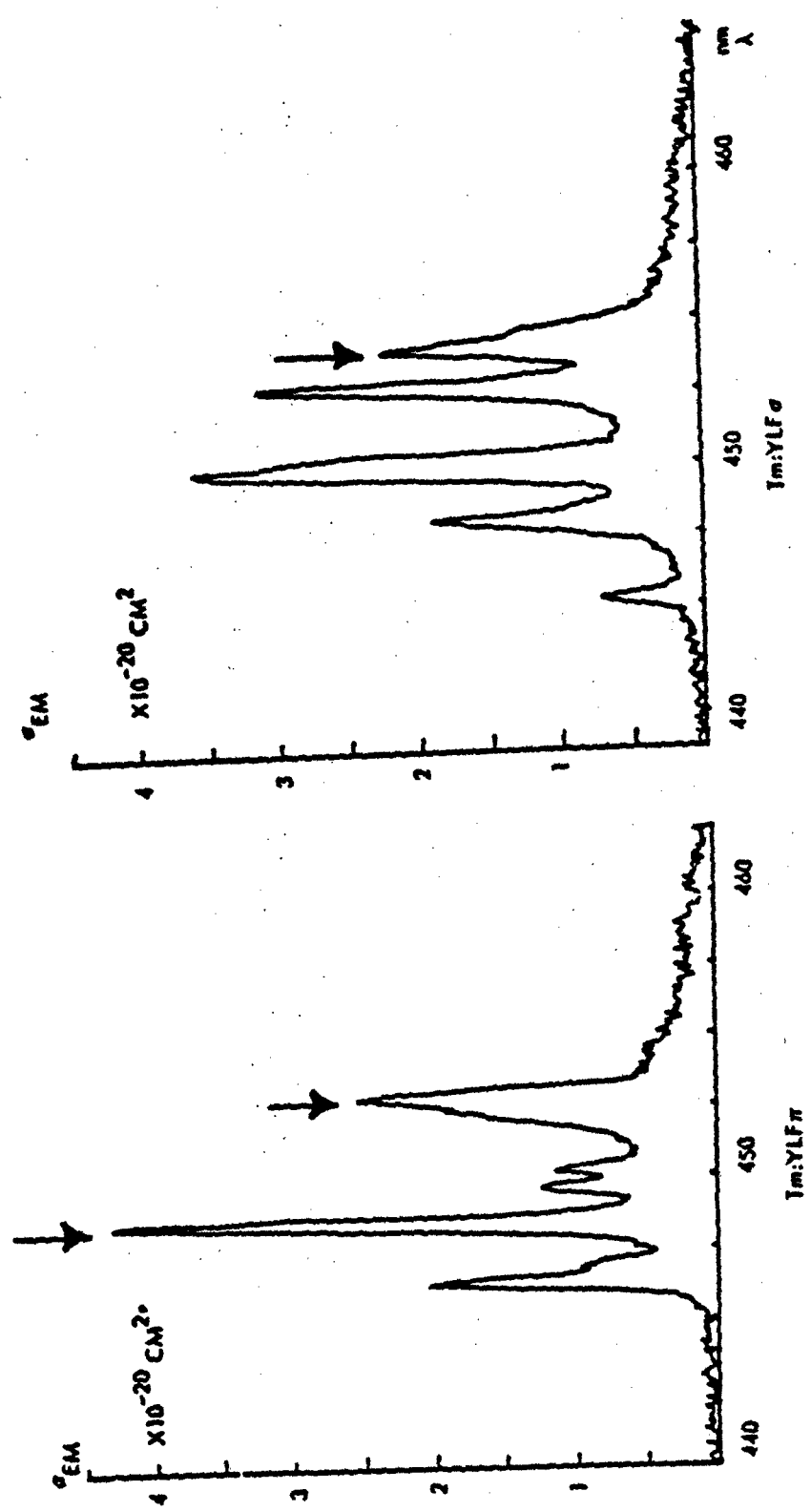


Figure 3-25

10230-3

4.0 SUMMARY AND CONCLUSIONS

The measured gain of a Tm:YLF amplifier operated in the small signal gain regime is in good agreement with the gain predicted by a "pump-while-extract" model using the measured values of fluorescence lifetime, pump absorption coefficient, stimulated emission cross-section and relevant experimental parameters. Further work is needed, however, to confirm these results as the experiments were, of necessity, crude. Experiments with a tripled Nd:YAG pump with a well controlled beam are recommended; and it would be useful in such experiments to develop an empirical value for the saturation fluence of the $^1D_2 - ^3F_4$ laser transition(s) in this material.

The absence of detectable loss due to $^3H_4 - ^3P_0$ excited state absorption in these small scale experiments, and the diminished magnitude of this loss mechanism in large aperture (low Tm concentration) crystals indicates that efficient extraction of the stored energy is possible in this material. Tm:YLF amplifiers appear to obey the Franz-Nodvik equation for a loss-less amplifier. Amplifier efficiency will be fundamentally limited by the photon decrement, upper and lower laser level occupation factors whose product is 61%⁽¹⁾ and Franz-Nodvik.

The properties of Tm³⁺:YLF permit the design of very high average power devices. The heat loading in the resonant pumped system can be as low as ~ 10-15% of the stored energy⁽¹⁾ compared to ~ 200% typical for flashlamp pumped solid state lasers. High average power face cooled disc amplifiers have been designed with near diffraction limited beam quality at output powers in the kilo-watt regime.⁽⁴⁾ Manzo,⁽⁵⁾ et al have designed multi-kilojoule - 10 Hz Tm:YLF active mirror modules with conversion efficiencies >40%. Such systems appear feasible; however further development of this technology is needed.

REFERENCES

1. E.P. Chicklis, et al., "High Power Laser and Materials Investigation" Final Report DOE-AC08-78DP40054, June 1980
2. E.P. Chicklis and J.Baer, "Rare Gas Halide Pumped Solid State Lasers" DOE Adv. Laser Meeting - W.J. Shaefer Associates, Inc., Report WJSA-78-6-SR-10, July 1979
3. M.G. Knights, et al., IEEE J. Quantum Electronics QE-18, No. 2, p. 163, February 1982
4. J.W. Baer, Sanders Associates, unpublished
5. P.R. Manzo, R. Schlecht, H. Verdun "An Analysis of the Potential of the Tm^{3+} :YLF:XeF Laser System as a Fusion Driver". Contract DOE-ED78-C-01-6456, Science Applications, Inc. Report #168-201-016, Feb. 1981

APPENDIX A

LASER AMPLIFIER MODEL

A simple computer simulation has been implemented. Approximating both the XeF and dye laser beams as uniform, plane waves with "top-hat" temporal profiles, the simulation is accomplished by running successive absorptions, decays and small signal gain passes on one nanosecond "slices" of each beam.

The required inputs to the program are the XeF pump energy, area and pulsewidth. The machine also needs to know the fraction absorbed by the crystal. Next, the dye laser energy, area and pulsewidth are required, along with the fraction of the blue beam that passes through the region. The delay between the beams is entered, as is the cross-section, fluorescent lifetime and upper and lower level occupation factors.

For each nanosecond, the program ascertains if the pump pulse has expired. If not, it adds one nanosecond fraction of the pump fluence to the crystal. It then allows the upper level to decay for one nanosecond. If the delay period is over, it passes a one nanosecond fraction of blue light through the crystal, calculating the gain by the small signal approximation. This is quite valid as the fluence in one nanosecond is usually $<.01 \text{ J/cm}^2$ on $<10^{-3} E_{\text{sat}}$. If the blue pulse has not ended, it goes back and does another loop.

The output energy is the product of the pumped area covered by the blue times the output fluence plus that blue light that bypasses the pumped region.

The program then calculates, rounds off and displays the output energy, that fraction of the output energy that represents energy converted from the UV. The conversion efficiency with regard to the

delivered UV beam and the change on a meter intercepting any part of the blue output beam.

Table A-1 includes a listing of the program from Sanders' DEC-20. The actual simulation arithmetic is located in lines 750-910. The rest is input/output and formatting.

TABLE A-1 PUMP-WHILE-EXTRACT PROGRAM LISTING

```

00100 DIM D(20),ES(20),GS(20)
00110 D(1)=2
00120 ES(1)="PUMP ENERGY"
00130 GS(1)="OP"
00140 D(2)=1000
00150 ES(2)="PUMP PULSEWIDTH"
00160 GS(2)="TP"
00170 D(3)=.2
00180 ES(3)="PUMP AREA"
00190 GS(3)="AP"
00200 D(4)=.30
00210 ES(4)="ABSORPTION"
00220 GS(4)="ABS"
00230 D(5)=.5
00240 ES(5)="SEED ENERGY"
00250 GS(5)="ES"
00260 D(6)=500
00270 ES(6)="SEED PULSEWIDTH"
00280 GS(6)="TS"
00290 D(7)=.2
00300 ES(7)="SEED AREA"
00310 GS(7)="AS"
00320 D(8)=.85
00330 ES(8)="OVERLAP"
00340 GS(8)="OVL"
00350 D(9)=1.2
00360 ES(9)="CROSS SECTION 4E-20"
00370 GS(9)="CS"
00380 D(10)=.171
00390 ES(10)="UPPER OCCUPATION"
00400 GS(10)="BU"
00410 D(11)=.049
00420 ES(11)="LOWER OCCUPATION"
00430 GS(11)="BL"
00440 D(12)=2140
00450 ES(12)="FLUORESCENT LIFETIME"
00460 GS(12)="TF"
00470 D(13)=500
00480 ES(13)="DELAY"
00490 GS(13)="TD"
00500 D(14)=0
00510 ES(14)="RUN"
00520 D(15)=0
00530 ES(15)="QUIT"
00540 D(16)=1
00550 ES(16)="FOR SHORT LIST HIT 0"
00560 GOTO 600
00570 FOR N=1 TO 15
00580 PRINT TAB(5);D(N);TAB(13);ES(N);TAB(10);GS(N)
00590 NEXT N
00600 PRINT "COMMANDS"
00610 INPUT P
00620 IF P=0 THEN GOTO 1010
00630 IF P=14 THEN GOTO 720
00640 IF P=15 THEN GOTO 400
00650 PRINT GS(P);" = ";D(P);" "
00660 INPUT D(P)
00670 GOTO 600
00680 PRINT "ARE YOU SURE?"
00690 INPUT Y$
00700 IF Y$="Y" THEN STOP
00710 GOTO 570
00720 RM=0
00730 RL=0
00740 RS=0
00750 PR=D(1)+D(4)+0.01778/(D(2)+D(3))
00760 DC=DO*(-1/D(12))
00770 DS=D(5)+0.02264/(D(6)+D(7))
00780 DLP=D(13)+D(4)
00790 SR=D(11)/D(10)
00800 PRINT
00810 FOR T=1 TO DLP
00820 IF T>D(2) THEN GOTO 040
00830 RM=RM+D
00840 RL=RL+DL
00850 IF T<D(13) THEN GOTO 910
00860 ETL=DO*((RM+RL+SR)+D(9))
00870 SD=SD+ST+EDL
00880 GR=DS+(EDL-1)
00890 RM=RM-SM
00900 RL=RL-SM
00910 NEXT T
00920 PRINT "OUTPUT":PRINT "INCREASE":PRINT "CONV EFF":PRINT "METER CHG"
00930 QD=SD+4.14+D(7)+D(8)+(1-D(4))+D(5)
00940 QI=INT(1000+QD-D(5))+0.5/1000
00950 QD=INT(1000+QD)/1000
00960 EFF=INT(1000+QI/D(1)+RL+SR)/10
00970 INC=INT(1000+QI-D(5))/10
00980 PRINT QD;" J":QI;" J":EFF;" %":INC;" %"
00990 GOTO
01000 GOTO 400
01010 FOR N=1 TO 13
01020 TB=D(N)
01030 IF N=3 THEN TB=TB-2
01040 IF N=6 THEN TB=TB-2
01050 PRINT TAB(TB);ES(N)
01060 NEXT N
01070 PRINT
01080 FOR N=1 TO 13
01090 TB=D(N)
01100 PRINT TAB(TB);D(N)
01110 NEXT N
01120 PRINT
01130 PRINT
01140 GOTO 400

```